Catalysis Science & Technology

Accepted Manuscript

This is an *Accepted Manuscript*, which has been through the Royal Society of Chemistry peer review process and has been accepted for publication.

Accepted Manuscripts are published online shortly after acceptance, before technical editing, formatting and proof reading. Using this free service, authors can make their results available to the community, in citable form, before we publish the edited article. We will replace this *Accepted Manuscript* with the edited and formatted *Advance Article* as soon as it is available.

You can find more information about *Accepted Manuscripts* in the Information for Authors.

Please note that technical editing may introduce minor changes to the text and/or graphics, which may alter content. The journal's standard Terms & Conditions and the Ethical guidelines still apply. In no event shall the Royal Society of Chemistry be held responsible for any errors or omissions in this *Accepted Manuscript* or any consequences arising from the use of any information it contains.

ROYAL SOCIETY OF CHEMISTRY

www.rsc.org/catalysis

Influence of calcination on performance of Bi-Ni-O/gamma-alumina catalyst for *n*-butane oxidative dehydrogenation to butadiene

B. Rabindran Jermy [1], S. Asaoka [1], S. Al-Khattaf [1,2]*

Abstract

Influence of calcination on the binary-metal oxide 30wt%Bi-20wt%Ni-O /gamma-Al_2O_3 catalyst was studied for n-butane oxidative dehydrogenation to 1,3-butadiene. The importance of the calcination was confirmed with the facts that 1) the two step calcination of more than 2 h at 2nd step resulted in higher activity and selectivity to butadiene and 2) the second step calcination temperatures showed clear effects on the activity and the selectivity. The activity showed a trend of volcano shape with the top at 590 ^{o}C at lower reaction temperature, 400 ^{o}C or a down-slope shape at 450 ^{o}C. As for the reaction selectivity, either the total dehydrogenation or the specific butadiene selectivity showed a volcano shape with the calcination temperature. The top along the calcination temperature existed at 590 ^{o}C in both cases of 400 ^{o}C and 450 ^{o}C reaction temperatures. Reversely, the selectivity of oxygenate formation (partially followed by cracking) or partial oxidation to CO/H_2 showed a valley shape with the bottom at 590 ^{o}C or 650 ^{o}C along the calcination temperature, respectively. The butadiene selectivity was more strongly influenced competitively by both of the oxygenate formation and the partial oxidation. From the catalyst characterization, it was observed that the redox and acid/base system (active and selective to the reaction) of the combined oxides with porous structure is formed as the cohabitation consisting of 'hierarchical nano-particles' (NiO, alpha-/beta-Bi_2O_3 and gamma-Al_2O_3) resulted from the catalyst calcination in a preferable condition.

Catalysis Science & Technology Accepted Manuscript

***Keywords*:** Oxidative dehydrogenation; *n*-butane; butadiene; nano-particle; calcination.

[1] *Center of Research Excellence in Petroleum Refining and Petrochemicals, King Fahd University of Petroleum & Minerals, Dhahran 31261, Saudi Arabia*

[2] *Department of Chemical Engineering, King Fahd University of Petroleum & Minerals, Dhahran 31261, Saudi Arabia*

Email: rabindra@kfupm.edu.sa, asataro4322@gmail.com, skhattaf@kfupm.edu.sa

Catalysis Science & Technology Accepted Manuscript

Research highlight

- Oxidative dehydrogenation of n-butane to butadiene was studied on Bi-Ni-O/gamma-alumina catalyst.
- Condition of catalyst calcination mainly effects on the selectivity.
- The calcination temperature results a volcano shape effect on the selectivity.
- The selective catalyst by calcination is consisting of hierarchical nano-particle cohabitation.

Catalysis Science & Technology Accepted Manuscript

Graphical abstract

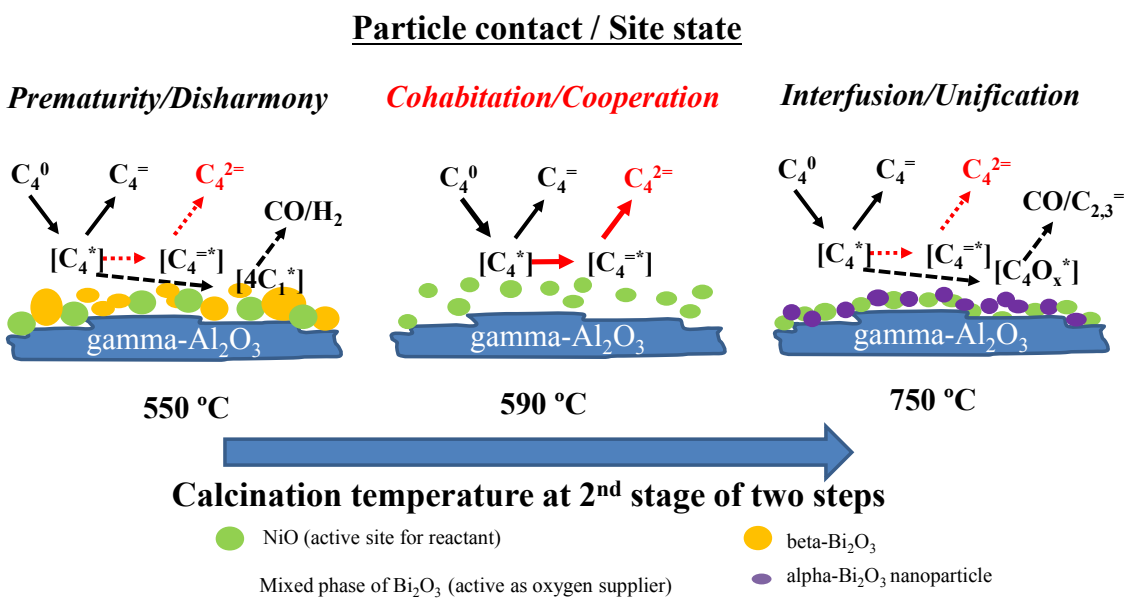

Catalysis Science & Technology Accepted Manuscript

Influence of calcination on performance of Bi-Ni-O/gamma-alumina catalyst for *n*-butane oxidative dehydrogenation to butadiene

B. Rabindran Jermy [1], S. Asaoka [1], S. Al-Khattaf [1,2]*

Abstract

Influence of calcination on the binary-metal oxide 30wt%Bi-20wt%Ni-O /gamma-Al_2O_3 catalyst was studied for n-butane oxidative dehydrogenation to 1,3-butadiene. The importance of the calcination was confirmed with the facts that 1) the two step calcination of more than 2 h at 2nd step resulted in higher activity and selectivity to butadiene and 2) the second step calcination temperatures showed clear effects on the activity and the selectivity. The activity showed a trend of volcano shape with the top at 590 ^{o}C at lower reaction temperature, 400 ^{o}C or a down-slope shape at 450 ^{o}C. As for the reaction selectivity, either the total dehydrogenation or the specific butadiene selectivity showed a volcano shape with the calcination temperature. The top along the calcination temperature existed at 590 ^{o}C in both cases of 400 ^{o}C and 450 ^{o}C reaction temperatures. Reversely, the selectivity of oxygenate formation (partially followed by cracking) or partial oxidation to CO/H_2 showed a valley shape with the bottom at 590 ^{o}C or 650 ^{o}C along the calcination temperature, respectively. The butadiene selectivity was more strongly influenced competitively by both of the oxygenate formation and the partial oxidation. From the catalyst characterization, it was observed that the redox and acid/base system (active and selective to the reaction) of the combined oxides with porous structure is formed as the cohabitation consisting of 'hierarchical nano-particles' (NiO, alpha-/beta-Bi_2O_3 and gamma-Al_2O_3) resulted from the catalyst calcination in a preferable condition.

Catalysis Science & Technology Accepted Manuscript

***Keywords*:** Oxidative dehydrogenation; *n*-butane; butadiene; nano-particle; calcination.

[1] *Center of Research Excellence in Petroleum Refining and Petrochemicals, King Fahd University of Petroleum & Minerals, Dhahran 31261, Saudi Arabia*

[2] *Department of Chemical Engineering, King Fahd University of Petroleum & Minerals, Dhahran 31261, Saudi Arabia*

Email: rabindra@kfupm.edu.sa, asataro4322@gmail.com, skhattaf@kfupm.edu.sa

1. Introduction

Butadiene (1, 3-butadiene: C_4H_6) is a major product for the petrochemical industry and the basis of a wide variety of synthetic rubbers, elastomers and polymer resins[1]. The butadiene is mainly obtained as a byproduct from naphtha crackers (ethylene plants). The butadiene is also produced by on-purpose production units, dehydrogenation of n-butane and n-butenes[2]. The growth of ethylene production has led to a shut-down of many on-purpose butadiene production units. But, recent trends in steam cracking show a lightened feedstock as the result of lower cost and larger availability of ethane from natural gas. The shale gas revolution probably more accelerates these trends. This change in feedstock shortens butadiene supply because of the lower butadiene yield from ethane relative to naphtha in the steam cracker. This worldwide change requests a new technology of on-purpose butadiene production.

In the existing on-purpose processes, n-butane and n-butenes based catalytic direct dehydrogenation is operated over chromium/alumina catalysts at temperature approximately 600-680 ^{o}C[3]. At such high operating condition, thermal cracking of hydrocarbon occurs and frequent catalyst regeneration is required due to coke deposition.

Catalysis Science & Technology Accepted Manuscript

In our previous work, supported Cr-V catalysts were investigated for direct dehydrogenation of n-butane to butadiene[4]. However, as this direct dehydrogenation requires high temperature operation due to thermodynamic equilibrium to butadiene, it inevitably causes the formation of excessive coke and quick deactivation of catalyst. Additionally, co-existence of carbon dioxide in the direct dehydrogenation over the supported Cr-V catalyst was also studied to lower the operation temperature with hydrogen removal by reverse water-gas shift reaction. The effect was still rather limited, as shown in our previous paper[5].

On the other hand, oxidative dehydrogenation with oxygen can be carried out at relatively lower reaction temperature. The process is not limited by thermodynamic equilibrium and the catalyst deactivation is reduced due to the presence of oxygen[6-8]. However, in oxidative dehydrogenation, selective oxidation of n-butane to 1, 3-butadiene is challenging. Higher temperature is required to activate n-butane relative to n-butenes, while dehydrogenated products (i.e. butenes and butadiene) react rapidly with oxygen to form unstable oxygenates and stable combustion products like carbon dioxide and water[7,9]. A suitable catalyst is needed to overcome this limitation by operating at relatively lower reaction temperature at lower O_2/n-C_4H_{10} ratio.

It has been generally recognized that the catalytic activity and selectivity for oxidative dehydrogenation are related to the redox property and surface acid-base character. For the redox property, the catalyst lattice oxygen participates in oxidation reaction for hydrogen and hydrocarbon intermediates. And then the reduced catalyst surface is restored to its earlier oxidation state by adsorption of oxygen from gas phase.

Catalysis Science & Technology Accepted Manuscript

The evolution of lattice oxygen is usually promoted by the interaction between metal oxides of the components[10]. A number of catalysts have been investigated for the oxidative dehydrogenation of n-butane to preferably butenes, including V-MgO[11-13], Ni-Mo-O[14, 15], MoO_3/MgO[16], titanium pyrophosphate[7] and V_2O_5/SiO_2[8]. In such catalytic systems, despite high dehydrogenation activity, selectivity with respect to butadiene is very low. For instance, it was reported over titanium pyrophosphate catalyst that the maximum n-butane conversion was of 28% and selectivity to dehydrogenation products was of 47%, while the formation of butadiene remained at about 14% and less compared to butenes (33%)[7]. It was reported over vanadia dispersed SiO_2 catalyst that the predominant reaction products were butenes (1-butene, trans and cis-2-butene), while 1, 3-butadiene product selectivity was minor (16%) along with cracking products[8].

In the previous literatures, most of the works are related to the oxidative dehydrogenation of n-butane mainly to butenes. In such cases, the selectivity to butenes occurs by inner C-H group activation of butane on the acid sites of catalyst surface. For selective butadiene formation, further activation of second C-H group of butenes is needed. In such case, the literature dealing with desired characteristics of catalyst (both acid and base) are limited and needed to be investigated.

Ni oxide/gamma-Al_2O_3 (hereafter gamma-Al_2O_3 will be used as Al_2O_3) based catalysts have attracted much attention for oxidative dehydrogenation of ethane to ethylene, where nickel sites seem to be the active sites for ethane activation[17-19]. The catalyst concept for the ethane oxidative dehydrogenation over Ni oxide/Al_2O_3 based catalysts was considered as also effective against an activation of methyl C-H bond at the

Catalysis Science & Technology Accepted Manuscript

end of n-butane and n-butenes.

Furthermore in recent years, bismuth oxides (Bi_2O_3) have been intensely investigated, due to their possible applications as oxygen-mobile oxides. The investigation revealed that Bi_2O_3 is less stable and the ionic conductivity depends on the type of Bi_2O_3 polymorph[20]. The ionic conductivity and stability against ageing can be improved significantly by doping Bi_2O_3 with other cations [21-23]. The addition of Bi_2O_3 component is critical for the formation of electrically active grain boundaries in the other oxide[24]. Chemical and microstructural properties of Bi_2O_3 depend on the synthesis method of Bi_2O_3[25-29].

Combining the above two background technologies, Bi-Ni oxide on Al_2O_3 was studied as catalyst for n-butane oxidative dehydrogenation to butadiene in our previous work[30]. 30wt%Bi-20wt%Ni-O/Al_2O_3 catalyst suppressed CO/H_2 production and showed high activity and selectivity. Bi addition to NiO results in a couple of weak acidity and moderate basicity with NiO dispersion and redox improvement. This manuscript is as for the follow-up research work based on the n-butane oxidative dehydrogenation. On the other hand, calcination is well-known as an important factor to influence the catalyst structure and properties, such as the dispersion of active sites[4, 5, 31-33], the interaction between metal oxide species and support[7, 34-36], as well as the acid-base properties [8, 9, 37-40].

The point of this manuscript is to study the effect of calcination condition. Among the programming rates from the room temperature to the target temperature the important

Catalysis Science & Technology Accepted Manuscript

conditions are temperature raising rate, the target temperature and the holding time. In this manuscript, the importance of temperature raising rate has been considered by examining the calcination steps instead of straight raising of temperature, simulated to the industrial procedure. One-step calcination as rapid temperature raising is compared to two-step calcination as slow temperature raising. Aiming at systematically investigating the influence of calcination on the 30wt%Bi-20wt%Ni/Al_2O_3 catalyst, effect of calcination (steps, time and temperature) on oxidative dehydrogenation performance was studied in the view of the catalyst character (structure, properties and oxide-support interactions), which has not been reported before.

First, an importance of the two step calcination was confirmed. Second, the effect of the second step calcination time was studied over a catalyst typically calcined at 590°C. Third, the second step calcination temperatures were precisely examined to focus on effects on the activity and the selectivity. Fourth, selectivity and reaction routes was discussed as for butadiene selectivity in dehydrogenation and selectivity correlation between 1st and 2nd dehydrogenation. Fifth, efficiency of oxidative hydrogen removal with oxygen usage was simulated. Finally, the catalytic performances due to the calcination were discussed, based on characterizations with XRD, TEM, TPR, surface area/pore structure and acid/base measurements to a different redox and acid/base property with porosity.

2. Experimental

2.1 Catalyst preparation

Catalysis Science & Technology Accepted Manuscript

The nano-sized porous Al_2O_3 (pore diameter: 9.8 nm, and pore volume: 0.83 ml/g) calcined at 550 ^oC was synthesized by successfully pH-controlled precipitation method using aluminum nitrate and sodium aluminate as precursors of boehmite and an acid–base pair of precipitating reagents according to detailed preparation technique as described by Kimura *et al.*[41-43].

The binary metal oxide Bi-Ni-O/Al_2O_3 catalysts were prepared by co-impregnation technique. Commercially available nickel nitrate hexahydrate $Ni(NO_3)_2{\cdot}6H_2O$ (99 %, Fisher Scientific) and bismuth nitrate pentahydrate $Bi(NO_3)_3{\cdot}5H_2O$ (98 %, Fluka-Garantie) were used as metal sources without further purification. For 30wt%Bi-20wt%Ni/Al_2O_3 catalyst, 9.8 g of nickel nitrate hexahydrate was dissolved in 800 ml of deionized water. After dissolution, 6.9 g of bismuth nitrate pentahydrate was added to the above solution and the resultant suspension was stirred for dissolution. Then 10.0 g of Al_2O_3 was added and kept in a closed vessel overnight for impregnation. After impregnation, the sample was dried at 120°C for 3 h to obtain an as-prepared catalyst.

For consistency between catalyst characterization and catalytic evaluation the as-prepared catalysts were served to the both experiments after activation and stabilization by calcination under flowing air. In one-step calcination, temperature was raised straightly from room temperature to 590 °C with the rate of 15 ^oC/min and kept for 2 h. In two-step calcination, the temperature was raised from room temperature to first step calcination temperature of 350 °C with the rate of 10 °C/min and held for 1 h. The temperature was raised again with rate of 15 °C/min until the second step target

Catalysis Science & Technology Accepted Manuscript

temperature of 590 °C and kept for 2 h. The calcination was carried out in the same system as the catalytic evaluation as shown below.

2.2 Catalytic evaluation

The catalytic runs were carried out in a fully integrated, fixed bed continuous-flow type reactor system (BELCAT). The system consists of one tubular quartz reactor attached with stainless steel one-zone furnace assembly through reactor furnace wall thermo well. The as-prepared catalyst sample (0.30 g) was packed in the reactor and pretreated to activate and stabilize as a catalyst under flowing air at higher temperature. The reaction test started after cooling-down to the reaction test temperature under flowing nitrogen. The flow rate of reactants (n-butane and air) and N_2 were controlled at appropriate proportions. In the study on the oxidative dehydrogenation, the oxygen to hydrocarbon ratio (O_2/n-C_4H_{10}) and temperature is considered to play a decisive role in the catalytic selectivity. The catalyst evaluation was operated selecting the reaction conditions at different temperatures (400 and 450 ^oC) and under different feed ratio of oxygen to n-butane (O_2/n-C_4H_{10} = 1 and 2 mol/mol).

Considering the exothermic nature of this oxidative dehydrogenation, the local temperature of catalyst bed was monitored by thermocouple inserted with thermocouple well. The effluent was analyzed online by using a GC system (Agilent, 7890N). One GC equipped with FID and GC-GasPro capillary column (L: 60 m and ID: 0.32 mm) was used to analyze hydrocarbons and oxygenates. The other GC with TCD and ShinCarbon 80/100 mesh SS column (He carrier) and MS5A 60/80 mesh SS column (Ar carrier) were used to detect the gases, N_2, O_2, CO and CO_2, and H_2, respectively. The products were

Catalysis Science & Technology Accepted Manuscript

identified by comparison with standard samples. Conversion of n-butane and selectivity to products were calculated based on the balance of carbon.

2.3 Catalyst characterization

The BET surface area and pore structure of the calcined catalysts were measured on a Micromeritics ASAP 2020 instrument (Norcross, GA). Before adsorption measurements, samples (ca. 0.1 g) were degassed at 240 °C for 3 h under nitrogen flow. The nitrogen adsorption isotherms were measured at liquid nitrogen temperature (−196 °C). Powder XRD analyses of the calcined catalysts were carried out using Rigaku Miniflex II desktop X-ray diffractometer in a diffraction angle (2θ) range of 5° to 80° with Cu Kα radiation (λ=1.5406 Å) at operating parameters of 30mA and 40kV with a step size of 0.02° and speed of 2°/min. The morphologies of the calcined catalysts were characterized by an advanced field emission transmission electron microscope (HRTEM-model JEM-2100F) with an acceleration voltage of 200 kV. The high-resolution images have been obtained on CCD camera and crystallographic information of oxide layers were obtained using Fast Fourier Transform (FFT) technique.

TPR and TPD (temperature-programmed reduction and desorption) experiments were performed in BEL-CAT-A-200 chemisorption apparatus. The equipment consists of quartz sample holder with high temperature furnace, and a pair of a thermal conductivity detector (TCD) and a mass spectrometer. The linearity of the TCD response was established by the injection of gas pulses of known volume in helium background flow. H_2-TPR analysis was performed using Ar/H_2 gas mixture (95/5 vol%). The total flow rate of the gas mixture was 50 cm^3/min. The sample (100 mg) was preheated in He at 300 °C

Catalysis Science & Technology Accepted Manuscript

for 3 h, and then cooled to room temperature. Then the sample was heated at 20 °C/min to the final temperature of 900 °C. The H_2 consumption was measured by a thermal conductivity detector and CuO was used as a reference for the calibration of H_2 consumption. Temperature programmed desorption of ammonia (NH_3-TPD) was carried out on the same instrument with substantially the same procedure to measure acidity. The procedure of NH_3-TPD is as follows. The calcined catalyst sample (100 mg) was pretreated regularly in a flow of He (50 mL/min) at 500 ^oC for 1 h. Then the sample was exposed to He/NH_3 mixture (95/5 vol%) at 100 °C for 30 min. The gas phase NH_3 was removed by He purging for 1 h followed by TPD, which was performed in He flow (50 mL/min) at a heating rate of 10 ^oC/min, and the desorbed NH_3 was monitored by either a TCD detector or a mass spectroscopy. Temperature programmed desorption of carbon dioxide (CO_2-TPD) was carried out on the same instrument with substantially the same procedure to measure basicity. In the case of CO_2-TPD, the gas phase is He/CO_2 mixture (95/5 vol%). The TGA-DTA curve was obtained by using TA, SDT Q600 instrument, at a heating rate of 10°C min^{-1} under nitrogen flow. The as-synthesized standard sample 30wt%Bi-20wt%Ni-O/Al_2O_3 was subjected to TGA-DTA analysis. The TGA showed main weight loss occurs around 350 ^oC (17%), and the second weight loss extends until 580 ^oC (5%).

3. Results and discussion

3.1 Catalytic evaluation

3.1.1 Comparison of calcination step number

The effects of calcination procedure, one step or two steps, on the activity as the conversion and the selectivity are shown in Table 1, summarizing 1) in low reaction

Catalysis Science & Technology Accepted Manuscript

temperature and low O_2/n-C_4H_{10} ratio case, 2) in low reaction temperature and high O_2/n-C_4H_{10} ratio case, and 3) in high reaction temperature and high O_2/n-C_4H_{10} ratio case. The precise product distributions for one step and two step sample 30wt%Bi-20wt%Ni-O/Al_2O_3 catalyst are provided as supporting data in Table s1. The main products in the effluent were obtained from dehydrogenation (DH: 1-butene, t-2-butene, cis-2-butene, 1,3-butadiene: BD), oxygenate formation with its cracking (OC: carboxylic acids and lighter olefins), and partial oxidation (PO: CO), while CO_2, CH_4, C_2H_6, C_3H_8 and the other oxygen-containing products were also detected as the negligible carbon-containing products by GC analysis. Scheme 1 shows the conversion route from the reactant to the products including co-product formation.

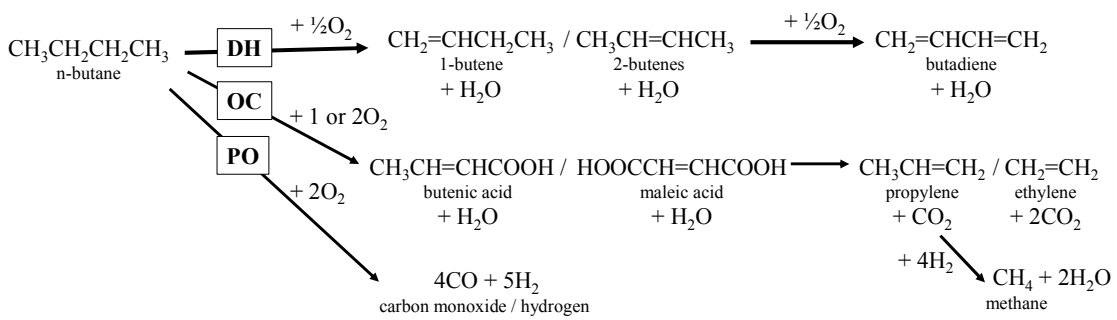

Scheme 1. Conversion route from the reactant to the products including co-product formation.

The carbon balance with oxygen and hydrogen balance of reaction data including Table 1 was checked by the GC of feed/product effluent, supported by the carbon content analysis of spent catalyst. The carbon balance was good in the case of high selectivity (two step), contrarily in the case of low selectivity (one step) less than 90 %. During the run,

Catalysis Science & Technology Accepted Manuscript

temperature increases of around 10 ^{o}C and 20 ^{o}C were observed in the cases of high and low selective catalysts, respectively.

First, Table 1 revealed that the two step calcination is superior to one step in any cases. Though the n-butane conversions are similar to one step in the cases of O_2/n-C_4H_{10} = 2 [mol/mol], total dehydrogenation selectivity (DH) and especially butadiene selectivity (BD) values are higher than one step calcination. Reversely, either oxygenate formation and the cracked (OC) or partial oxidation (PO) is nearly half relative to one step calcination. Therefore, the first step calcination at 350 ^{o}C for 1 h in the series of two step calcination holds an important role to the Bi-Ni-O/Al_2O_3 catalyst pretreatment so that it cannot be skipped.

Table 1 Comparison between one step and two step calcination to catalyst performance

Reaction temperature [ºC]	**400**		**400**		**450**	
O_2/n-C_4H_{10} [mol/mol]	**1**		**2**		**2**	
Catalyst calcination step[a]	**one**	**two**	**one**	**two**	**one**	**two**
C_4H_{10} conversion [%]	**11.8**	**14.1**	**18.4**	**18.3**	**25.9**	**26.9**
(O_2 conversion)	**(34.8)**	**(30.0)**	**(38.2)**	**(26.5)**	**(60.2)**	**(43.6)**
Selectivity[b] [C%]						
DH	**66.8**	**79.8**	**58.7**	**77.5**	**54.3**	**74.8**
(BD)	**(9.1)**	**(28.8)**	**(10.2)**	**(29.0)**	**(18.1)**	**(39.0)**
OC	**30.0**	**19.3**	**38.2**	**21.1**	**43.9**	**24.1**
PO	**3.2**	**0.8**	**3.2**	**1.3**	**1.8**	**1.1**
BD/DH [%]	**13.5**	**36.1**	**17.4**	**37.4**	**33.1**	**52.2**

[a]one step: 590ºC-2h, two step: 350ºC-1h+590ºC-2h
[b]DH: dehydrogenation, BD: butadiene, OC: oxygenate and the cracked, PO: partial oxidation.

Catalysis Science & Technology Accepted Manuscript

3.1.2 Effect of calcination time

Based on the performance as shown in Table 1, two step calcination was chosen as the standard calcination method to study the effect of calcination time. The 1st step calcination was maintained at 350 ^{o}C for 1 h, while 2nd step calcination at 590 ^{o}C was subsequently varied as 1, 2, 3 and 4 h, respectively.

The catalytic performances of catalyst after the 1st calcination (0 h) was not shown considering the required stabilization of bimetal oxide catalyst at this high temperature reaction conditions (400-500 ^{o}C). Sufficient calcination temperature is required to convert nitrate reagent to oxide form. Calcination at 0 h may still contain some unconverted nitrate active species and such system showed unstable catalytic performance. In addition, the active nitrate species may cause corrosive hazard and explosion at industrial scale. Fig. 1, 2 and 3 show the butane conversion and the product selectivity with the 2nd step calcination time 1) in low reaction temperature and low O_2/n-C_4H_{10} ratio case, 2) in low reaction temperature and high O_2/n-C_4H_{10} ratio case, and 3) in high reaction temperature and high O_2/n-C_4H_{10} ratio case, respectively. Except for 1 h calcination, the conversion and selectivity are nearly constant at a higher level relative to 1 h calcination. The performance of 1 h calcination catalyst is inferior to 2 h calcination. The degree of inferiority is larger than one step calcination. For example, though the three calcination methods show similar n-butane conversion, 1 h calcination shows DH: 51.9 C% and BD: 13.2 C%, on the contrary one step calcination and 2 h calcination show DH: 54.3 C% and BD: 18.1 C%, DH: 74.9 C% and BD: 39.0 C%, respectively in high reaction temperature and high O_2/C_4H_{10} ratio case. Time on stream of the reaction for 10 h was measured. The

Catalysis Science & Technology Accepted Manuscript

catalytic activity and selectivity were stable, especially as for the standard catalyst of the two step calcination shown in Table 1. The XRD analysis of spent catalyst in the time on stream run showed no difference from the fresh one, which indicates the good stability of the present catalyst system. Therefore, 2nd step calcination time becomes more important and two hours of time are enough to obtain the high performance of the catalyst.

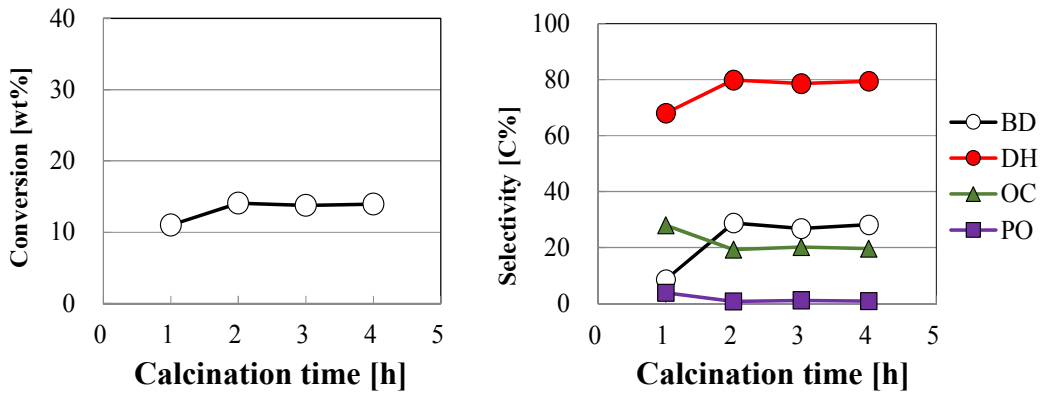

Fig.1 Effect of calcination time at 590 °C on the performance in low reaction temperature and low O_2/n-C_4H_{10} ratio case, catalyst: 30wt%Bi-20wt%Ni-O/Al_2O_3, reaction condition: 400 °C, O_2/n-C_4H_{10}=1 [mol/mol].

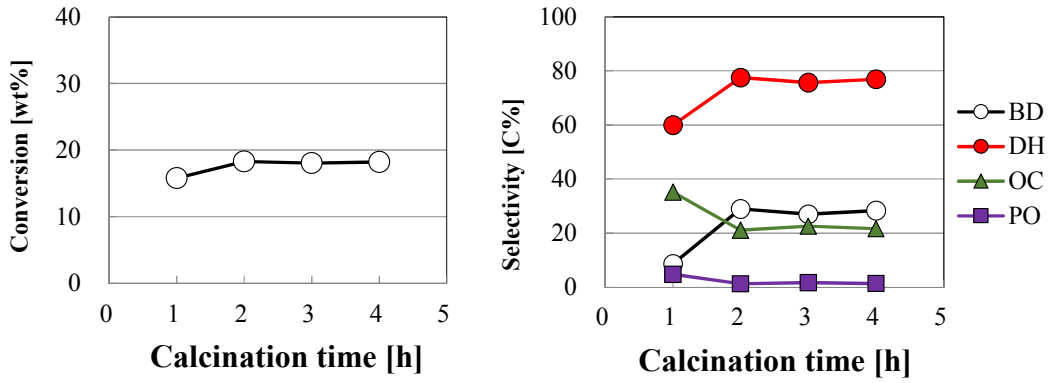

Fig.2 Effect of calcination time at 590 °C on the performance in low reaction temperature and high O_2/n-C_4H_{10} ratio case, catalyst: 30wt%Bi-20wt%Ni-O/Al_2O_3,

Catalysis Science & Technology Accepted Manuscript

reaction condition: 400 °C, O_2/n-C_4H_{10}=2 [mol/mol].

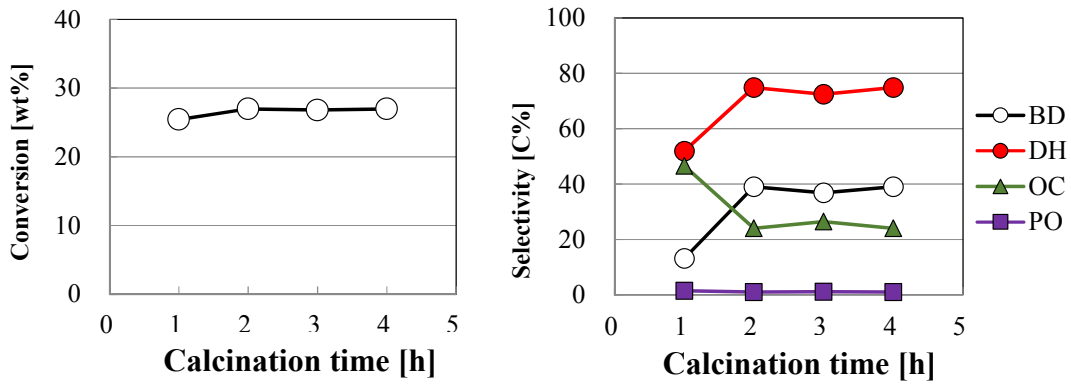

Fig.3 Effect of calcination time at 590 °C on the performance in high reaction temperature and high O_2/n-C_4H_{10} ratio case, catalyst: 30wt%Bi-20wt%Ni-O/Al_2O_3, reaction condition: 450 °C, O_2/n-C_4H_{10}=2 [mol/mol].

3.1.3 Dependency on calcination temperature

Based on the performance as shown in Table 1 and Fig. 1-3, two step and 2 h calcination was chosen as the standard calcination method to study the effect of calcination temperature. The 1st step calcination was maintained at 350 °C for 1 h and the 2nd step calcination time was also kept for 2 h, while 2nd step calcination was subsequently varied among 550, 590, 650, 700 and 750 °C. Fig. 4, 5 and 6 show the butane conversion and the product selectivity with the 2nd step calcination temperature 1) in low reaction temperature and low O_2/n-C_4H_{10} ratio case, 2) in low reaction temperature and high O_2/n-C_4H_{10} ratio case, and 3) in high reaction temperature and high O_2/n-C_4H_{10} ratio case, respectively.

The second step calcination temperatures showed clear effects on the activity and

Catalysis Science & Technology Accepted Manuscript

the selectivity. The activity showed an effect of a volcano shape with the top of 590 ^{o}C at lower reaction temperature, 400 ^{o}C, in both cases of low and high O_2/n-C_4H_{10} ratio, as slope shape as shown in Fig. 6. The effect was more clearly shown on the reaction selectivity as shown in Fig. 4, 5 and 6. Either the total dehydrogenation or the specific butadiene selectivity showed a volcano shape with the calcination temperature in all three cases. The top along the calcination temperature existed at 590 ^{o}C in both O_2/n-C_4H_{10} ratio cases at 400 ^{o}C. And this shape became clearer in 450 ^{o}C reaction temperature case, as shown in Fig. 6. Reversely, the selectivity of oxygenate formation partially followed by cracking such as carboxylic acids showed a half valley shape with the bottom at 550 to 590 ^{o}C along the calcination temperature in both O_2/n-C_4H_{10} ratio cases at 400 ^{o}C, and this shape became a clear valley with the bottom at 590 ^{o}C in reaction temperature 450 ^{o}C case, as shown in Fig. 6. The partial oxidation to CO and molecular hydrogen, while it is a minor reaction, behaved as the selectivity in the valley shape with the bottom at 650 ^{o}C along the calcination temperature in all three cases, as shown in Fig. 4, 5 and 6. The total selectivity of dehydrogenation was competitively influenced by the oxygenate formation and partial oxidation. The butadiene selectivity was more strongly influenced competitively not only by the oxygenate formation but also by the partial oxidation.

Catalysis Science & Technology Accepted Manuscript

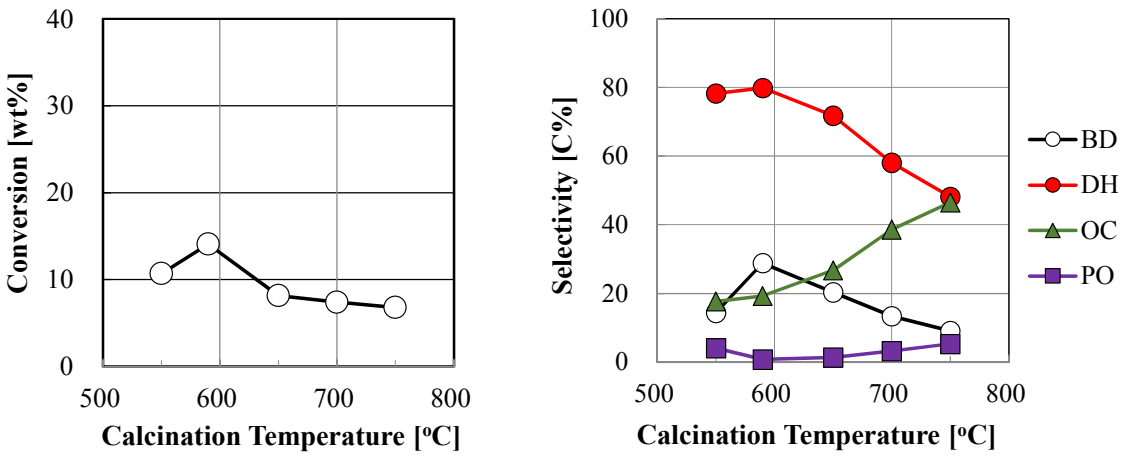

Fig.4 Effect of calcination temperature of 2nd step for 2 h on the performance in low reaction temperature and low O_2/n-C_4H_{10} ratio case, catalyst: 30wt%Bi-20wt%Ni-O/Al_2O_3, reaction condition: 400 °C, O_2/n-C_4H_{10}=1 [mol/mol].

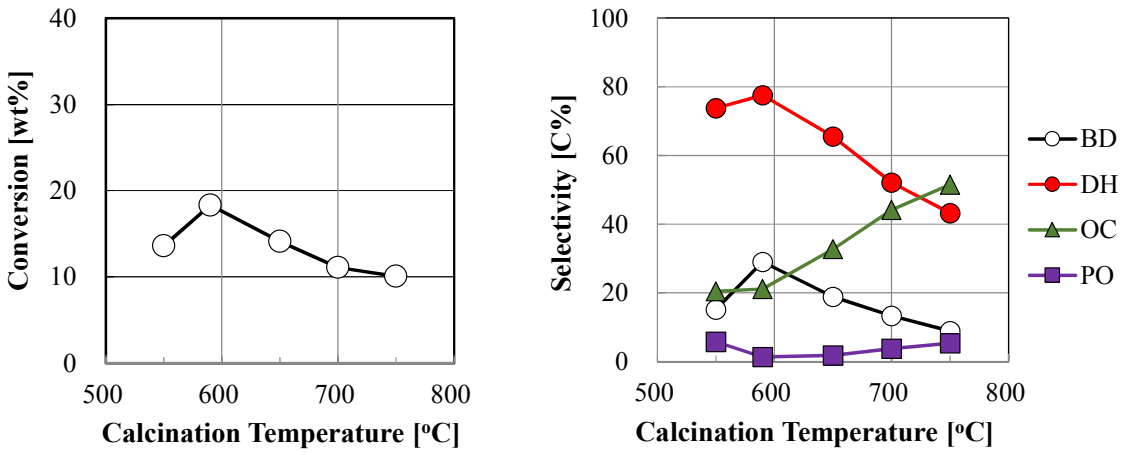

Fig.5 Effect of calcination temperature of 2nd step for 2 h on the performance in low reaction temperature and high O_2/n-C_4H_{10} ratio case, catalyst: 30wt%Bi-20wt%Ni-O/Al_2O_3, reaction condition: 400 °C, O_2/n-C_4H_{10}=2 [mol/mol].

Catalysis Science & Technology Accepted Manuscript

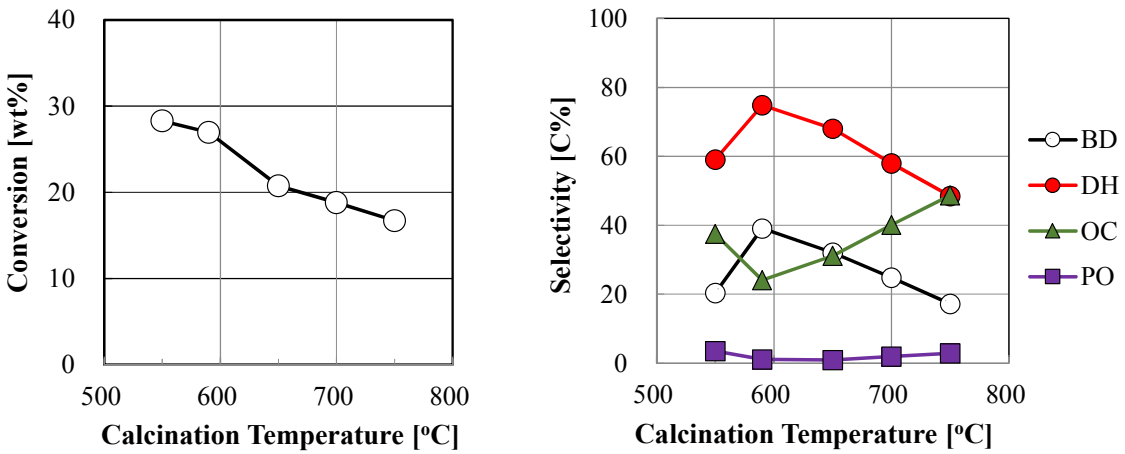

Fig.6 Effect of calcination temperature of 2nd step for 2 h on the performance in high reaction temperature and high O_2/n-C_4H_{10} ratio case, catalyst: 30wt%Bi-20wt%Ni-O/Al_2O_3, reaction condition: 450 °C, O_2/n-C_4H_{10}=2 [mol/mol].

3.1.4 Selectivity and reaction routes

1) Butadiene selectivity in dehydrogenation

In order to investigate further on reaction pathway over the Bi-Ni oxide/Al_2O_3 catalyst, the effect of calcination condition on the activity and selectivity was analyzed by relation between selectivity data with the viewpoint from butadiene production (second step dehydrogenation) in high reaction temperature (450 °C) and high O_2/n-C_4H_{10} ratio (2 mol/mol) case. The 2nd step dehydrogenation selectivity (butadiene selectivity to total dehydrogenation selectivity: BD/DH) were summarized to show as Fig. 7. As shown in Fig. 7, two step calcination made BD/DH higher than one step calcination did. The 2 h (and more than) calcination also made BD/DH higher than 1 h calcination did. Along increase of calcination temperature BD/DH showed a volcano shape with the top at 590

Catalysis Science & Technology Accepted Manuscript

^{o}C. The behaviors of BD/DH shown in Fig. 7 are close to the curves of total dehydrogenation selectivity (DH) with calcination time and with calcination temperatures shown in Fig. 3 and 6, respectively. These results suggest that the 2nd step dehydrogenation selectivity is closely related to the 1st step dehydrogenation selectivity controlled by the active site on the catalyst.

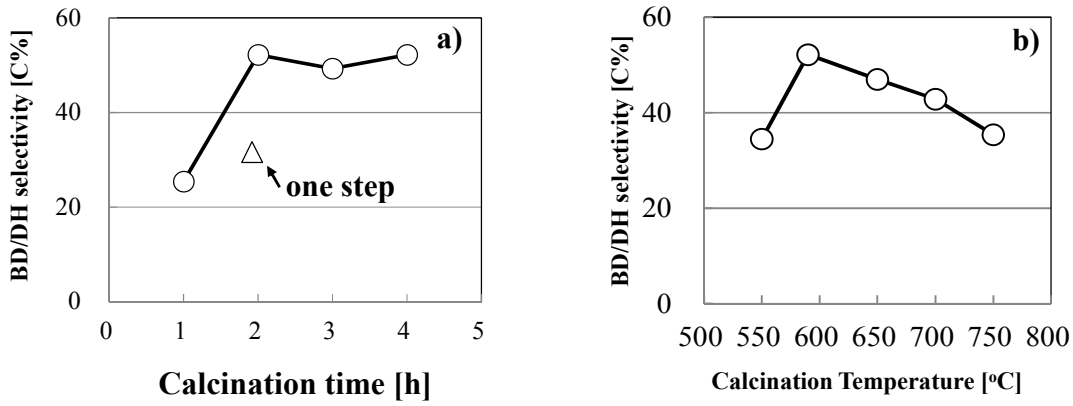

Fig.7 2nd step dehydrogenation selectivity to total dehydrogenation with calcination condition, a) time, b) temperature, catalyst: 30wt%Bi-20wt%Ni-O/Al_2O_3, reaction condition: 450 ^{o}C, O_2/n-C_4H_{10} = 2 [mol/mol].

2) Selectivity correlation between 1st and 2nd dehydrogenation

In order to investigate further on the active site controlling the 1st and 2nd step dehydrogenation selectivity over the Bi-Ni oxide/Al_2O_3 catalyst, DH product composition were precisely examined with the viewpoint of butene intermediate for butadiene formation. Referring to existing technology where 1-butene is claimed as the most preferable feedstock to butadiene production from mixed butenes, 2nd step of butadiene production was set up as the route:

1-butene CH_2=CH-CH_2-CH_3 → butadiene CH_2=CH-CH=CH_2.

Catalysis Science & Technology Accepted Manuscript

Therefore, to see if the following hypotheses reaction route:

Butane (C_4^0): CH_3-CH_2-CH_2-CH_3 → 1-butene ($C_4^=$): CH_2=CH-CH_2-CH_3

→ butadiene ($C_4^{2=}$): CH_2=CH-CH=CH_2.

The dehydrogenation activity and selectivity in the case of using 1-butene, which is the intermediate of the n-butane dehydrogenation, as the starting material were determined. As the result in the case of 1-butene feed, high reactivity with high BD selectivity was observed as shown in Table 2. As for the butadiene selectivity of 1-butene feed, the selectivity BD/(1-butene + BD) in Table 2 were determined to the hypothesized selectivities (1-butene + BD)/DH for 1st step and BD/(1-butene + BD) for 2nd step of n-butane feed.

Table 2 Comparison between n-butane and 1-butene feedstock to catalyst performance

Reaction temperature [ºC]	**400**		**400**		**450**	
O_2/Reactant [mol/mol]	**1**		**2**		**2**	
Reactant[a]	**n-C_4H_{10}**	**1-C_4H_8**	**n-C_4H_{10}**	**1-C_4H_8**	**n-C_4H_{10}**	**1-C_4H_8**
Reactant conversion [%]	**14.1**	**75.0**	**18.3**	**81.5**	**26.9**	**82.1**
Selectivity[b] [C%]						
DH	**79.8**	**91.0**	**77.5**	**85.4**	**74.8**	**85.5**
1-C_4H_8	**18.9**	**(-)**	**19.9**	**(-)**	**14.1**	**(-)**
BD	**28.8**	**32.8**	**29.0**	**40.6**	**39.0**	**37.8**
OC	**19.3**	**8.6**	**21.1**	**13.9**	**24.1**	**12.4**
PO	**0.8**	**0.4**	**1.3**	**0.7**	**1.1**	**2.1**
BD/(1-C_4H_8 + BD) [%]	**60.4**	**49.6**	**59.3**	**64.1**	**73.4**	**63.4**
(1-C_4H_8 + BD)/DH∗ [%]	**59.8**	**36.1**	**63.1**	**47.6**	**71.0**	**44.2**

[a] Catalyst: 30wt%Bi-20wt%Ni/Al_2O_3 calcined by two steps (350ºC-1h+590ºC-2h).
[b]DH∗: dehydrogenation + isomerization, BD: butadiene, OC: oxygenate and the cracked, PO: partial oxidation.

Catalysis Science & Technology Accepted Manuscript

Based on the result in Table 2 and returned to the selectivity of n-butane feed case, the equation: BD/(1-butene + BD) =A* (1-butene + BD)/DH (A=Coefficient) was considered by selectivity plotting 'butadiene selectivity of 2nd step against 1st dehydrogenation selectivity of 1-butene vs 1-butene selectivity of 1st dehydrogenation' as shown in Fig. 8.

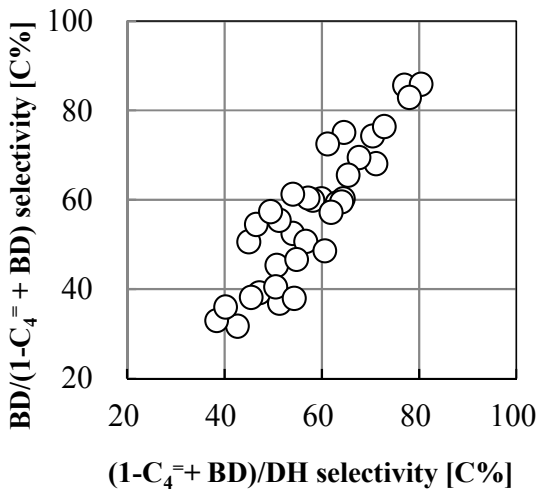

Fig.8 Selectivity correlation between 1st step and 2nd dehydrogenation in the case of butadiene formation via 1-butene route.

Fig. 8 suggests that 2nd step butadiene selectivity against 1-butene selectivity of 1st dehydrogenation is nearly not only proportional but also equal to 1-butene selectivity of 1st dehydrogenation, which means A = 1 in the above equation. This fact suggests the dehydrogenation of 1st step and 2nd step starts at the similar activated position of the reactant on the same active site of catalyst. As for such couple of position and site, withdrawing proton from terminal methyl position of the reactant is known as the basic

Catalysis Science & Technology Accepted Manuscript

catalyst site. Since BD/DH is simulated by using the following equation: BD/DH = 100 × [(1-butene + BD)/DH]^2, the 2nd step selectivity BD/DH can be increased by enforcement of the coupled functions for 1st step selectivity to 1-butene.

3.2 Catalyst characterization

3.2.1 Surface area and pore structure

The characterization of the catalyst might also provide valuable information to determine the state of active site, for example nickel species, i.e. metallic or oxidized. The state of Ni species of the catalyst was confirmed by TEM and color to be stably oxidized (subnano-sized NiO and light green: Ni^{2+}, respectively). The color was not changed even after 10 hours-on-stream of the reaction test. With respect to the activity and the selectivity, they are also stable without any results suggesting change of the catalyst characteristics as far as the catalysts were tested. In general as for more than 20 wt% Ni loaded Al_2O_3 catalyst, the presence of dark gray or black color indicates the reduction of Ni^{2+} to Ni^0. Therefore, the characterization of the calcined (just after calcination at more than 550°C for stabilization) catalysts themself is considered sufficient to give valuable information about catalytic character.

First, the BET surface area and pore structure (pore surface area, pore volume and average pore diameter) of Al_2O_3 support and the Bi-Ni-O/Al_2O_3 catalysts calcined at various temperatures are presented in Table 3. The catalyst support, Al_2O_3 (calcined at 550 ^{o}C) showed the BET surface area of 276 m^2/g. All catalysts exhibited lower BET surface area based on catalyst weight than Al_2O_3 support itself and they showed values decreased significantly with increase of calcination temperature to 100 m^2/g-catalyst.

Catalysis Science & Technology Accepted Manuscript

Pore surface area and pore volume based on catalyst weight also behaved with increase of calcination temperature similar to BET surface area. But, since all catalysts were loaded to Al_2O_3 support with 30wt%Bi and 20wt%Ni as oxides, the discussion about changes of the BET surface area and pore structures (pore surface area, pore volume and pore diameter) with calcination temperature should be based on the unloaded values (relative values to the catalyst volume based). The values based on weight of Al_2O_3 support were calculated to show at the next column of catalyst weight based one in Table 3. The catalysts calcined at 550 ^oC and 590 ^oC showed higher values, 359 and 351 m^2/g-Al_2O_3 of BET surface area than Al_2O_3 support, 276 m^2/g, respectively. They also showed higher values, 424 and 408 m^2/g-Al_2O_3 of pore surface area than Al_2O_3 support, 338 m^2/g, respectively. They similarly showed higher values, 1.02 and 1.08 ml/g-Al_2O_3 of pore volume than Al_2O_3 support, 0.83 ml/g, respectively.

These results suggest that the impregnated metal oxides formed not only additional surface area but also new pore space leading to pore volume increase. These phenomena are considered like pore expansion, so-called as 'super-impregnation', by nano-crystalized metal oxide in nano-sized pore. It becomes clearer by the fact that the catalyst calcined at 590 ^oC showed increased average pore diameter relative to the original Al_2O_3. Reversely, the catalysts calcined at more than 650 ^oC showed the decreased values not only relative to the original Al_2O_3 but also along with increase of calcination temperature.

Catalysis Science & Technology Accepted Manuscript

Table 3. BET surface area and pore structure of Al_2O_3 and Bi-NiO/Al_2O_3 catalysts.

Calcination temperature	BET surface area		Pore surface area		Pore volume		Average pore diameter
[ºC]	[m^2/g-catal][a]	[m^2/g-Al_2O_3][b]	[m^2/g-catal][c]	[m^2/g-Al_2O_3][d]	[m^2/g-catal][e]	[m^2/g-Al_2O_3][f]	[nm][g]
(Support: Al_2O_3)	276		338		0.83		9.8
550	226	359	267	424	0.64	1.02	9.5
590	221	351	257	408	0.68	1.08	10.6
650	153	243	179	284	0.40	0.63	8.9
700	146	232	171	272	0.40	0.63	9.3
750	100	159	117	186	0.30	0.47	10.1
590∗	166	264	200	318	0.51	0.81	10.2

∗One step calcination at 590 ºC, [a]BET surface area, [c,e,g]Surface area, pore volume and average pore diameter measured using BJH isotherm, [b,d,f]Surface area and pore volume calculated by volume based Al_2O_3 using the equation: SA or PV×[Σ(MO_x/M)+100]/100, where M=metal wt%; MO_x=metal oxide wt%; SA = Surface Area; PV = Pore Volume, [g]Average pore diameter = 4000×PV/SA.

Furthermore, the trends mentioned above are clearer when pore structure was break down as pore distribution as shown in Fig. s1. The figure is also plotted by 2 ways, i.e. the catalyst weight based and the Al_2O_3 weight based. Table 3 with Fig. s1 shows pore volume increases in the catalyst calcined at 550 ^oC and 590 ^oC occurred at pore diameter of 8 nm and 10 nm, respectively. Some crystal growth probably occurred from 550 ^oC to 590 ^oC of calcination temperature to make pore diameter larger. And from 650 ^oC to 750 ^oC of calcination temperature the crystal size reduction with Al_2O_3 sintering caused the shrinkage of pore volume, and reversely the increase of average pore diameter due to increase of pore volume at ca. 15 nm. The larger pore was probably made of the

Catalysis Science & Technology Accepted Manuscript

expanded nano-crystal ruin after sintering. Additionally, one step calcination did not cause some expansion but still stayed with a similar pore structure to original Al_2O_3 support, suggesting another crystallization pathway different from two step calcination. The above suppositions and considerations were discussed further by using mainly XRD and partly TEM measurements.

3.2.2 X-ray Diffraction

The X-ray diffraction (XRD) patterns for bismuth-nickel impregnated samples calcined in various conditions, 1 step or 2 step, different calcination time and temperatures are shown in Figs. 9, 10 and 11, respectively. As the reference XRD patterns, Fig. 9 includes the 30wt%Bi-O/Al_2O_3 catalyst (without Ni loading) and Fig. 11 includes the 620 ^oC calcined. Though XRD patterns were measured in a diffraction angle (2θ) range of 5° to 80° with Cu Kα radiation (λ=1.5406 Å), these figures are intentionally displayed only in 2θ range of 25° to 35° to precisely discuss on Bi_2O_3 phase transition resulting characteristic peaks in this range. XRD patterns of these samples were identified using data from JCPDS Powder Diffraction File[44]. One step or 1 h calcination at 590 ^oC resulted XRD patterns corresponded to the powder data for tetragonal β-Bi_2O_3, as shown in Fig. 9 and 10, respectively. XRD patterns recorded for catalysts calcined at various temperatures corresponded to a mixture of monoclinic α-Bi_2O_3 and tetragonal β-Bi_2O_3 in less than 700 ^oC of calcination temperature or a single phase component of α-Bi_2O_3 in 700 ^oC and 750 ^oC, as shown in Fig. 11. The crystallinity (peak height) and crystal size (reverse of half-height width) of α-Bi_2O_3 shown in the catalyst calcined at 750 ^oC became lower and smaller than these in the catalyst calcined at 700 ^oC. In this temperature region,

Catalysis Science & Technology Accepted Manuscript

NiO probably solves into Bi_2O_3 to make its crystal smaller. As for the catalysts calcined at less than 700 ^oC, the mixed phase composition of monoclinic and tetragonal Bi_2O_3 i.e. alpha-phase and beta-phase, were measured with deconvolution by using peaks of 700 ^oC calcined and one step calcined as two standards of single phase alpha-Bi_2O_3 and single phase beta-Bi_2O_3, respectively. The typical example of the deconvolution result is shown in supporting data (Fig.s2). The catalysts calcined at 550 ^oC, 590 ^oC, 620 ^oC and 650 ^oC contain 10%, 40%, 50% and 75% of Bi_2O_3 as alpha-phase, respectively, and the remains as beta-phase. Bi_2O_3 of the most selective catalyst, i.e. the 590 ^oC calcined has a phase composition of alpha-Bi_2O_3: 40% and beta-Bi_2O_3: 60%. Furthermore, since NiO peak from any 30wt%Bi-20wt%Ni-O/Al_2O_3 catalysts was not observed relative to 20wt%Ni-O/Al_2O_3 catalyst, the NiO was considered to be more highly dispersed than NiO (crystal size by XRD: ca. 3 nm) of 20wt%Ni-O/Al_2O_3 catalyst. Additionally, since 30wt%Bi-O/Al_2O_3 catalyst showed nearly single phase beta-Bi_2O_3 as shown in Fig. 9, the highly dispersed NiO probably works as a promoter to the Bi_2O_3 phase transition. The one step calcination may not permit Ni species promoting the Bi_2O_3 phase transition. In spite of well-known fact that Ni species are reducible in dispersion, we couldn't detect enlarged NiO particle or reduced Ni metal particle in spent catalyst by XRD. Nickel species are supposed to be exist as nanoparticle less than 3 nm, which are too small to be measured by XRD (detection limit). These considerations were confirmed by TEM observation on the states of Bi_2O_3 and NiO in the most selective catalyst, 30wt%Bi-20wt%Ni-O/Al_2O_3 catalyst calcined at 590 ^oC for 2 h.

The structure change of Bi_2O_3 was not clearly detected at 2nd calcination temperature by using DTA since the exothermic broad-shoulder peak was difficult to be

Catalysis Science & Technology Accepted Manuscript

exactly assigned to the structure change. It is supposed due to the condition of TGA-DTA analysis using N_2 atmosphere in spite of calcination condition using air atmosphere (Fig.s3).

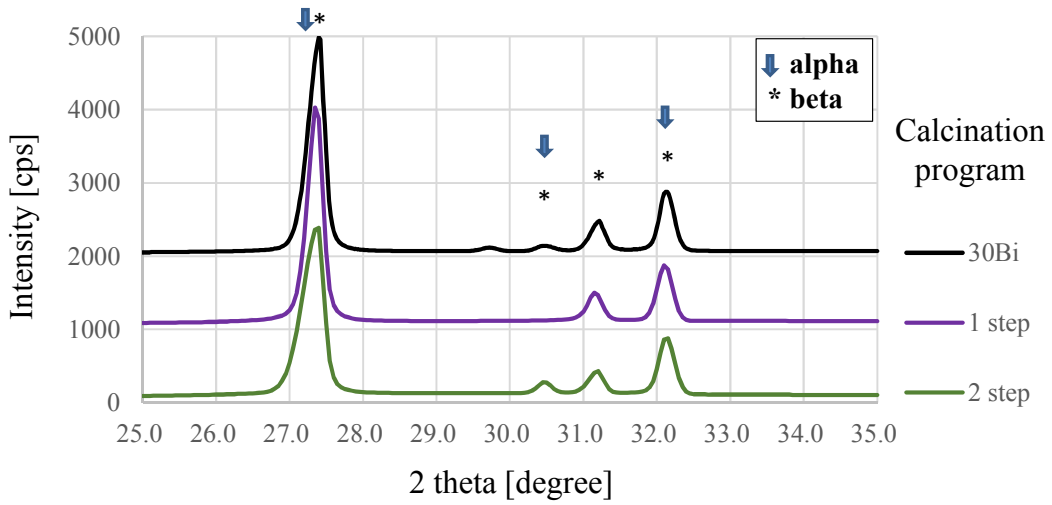

Fig.9 XRD comparison between 1 step and 2 step calcination

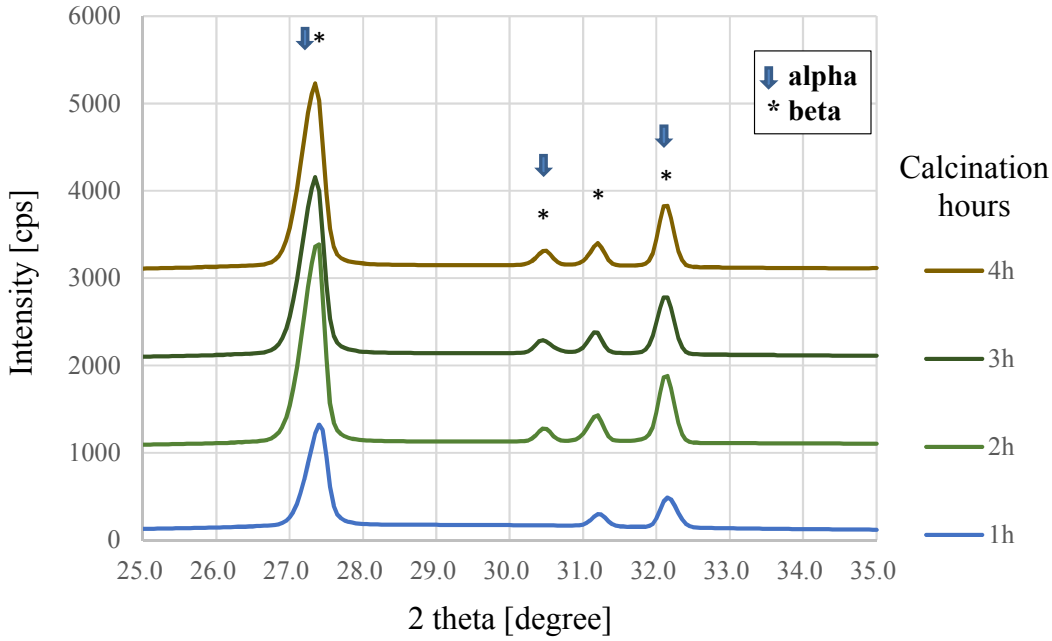

Fig.10 XRD comparison among calcination time

Catalysis Science & Technology Accepted Manuscript

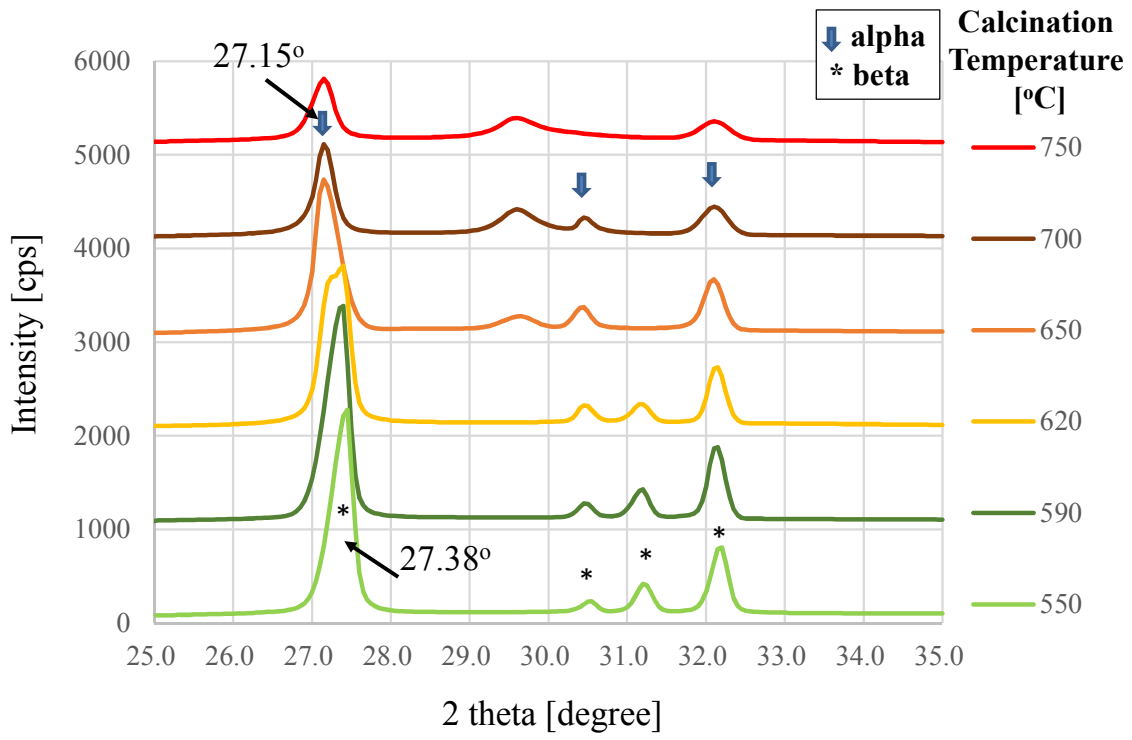

Fig.11 XRD comparison among calcination temperatures

3.2.3 TEM observation

The results of TEM observation on nickel and bismuth-nickel impregnated catalysts, 20wt%Ni-O/Al_2O_3 and 30wt%Bi-20wt%Ni-O/Al_2O_3 are shown in supporting data Fig s4 and Figs. 12(a-c), respectively. Both catalysts were calcined in the standard condition (at 350 °C for 1h followed by 590 °C for 2 h under flowing air). Figs. 12 (a and b) commonly show that nano-particles of Al_2O_3 support are stacked nano-particles with ca. 10 nm length, ca. 3 nm thickness and fractal shape, consisting of finer rods and slabs. Fig. s4 shows that NiO nano-particles of 20wt%Ni-O/Al_2O_3 catalyst are dispersed mainly as chained aggregates with ca. 3.0 nm diameter at the edge of the stacked Al_2O_3 nano-particles, in agreement with XRD measurement result. Contrarily, Figs. 12 (a-c)

Catalysis Science & Technology Accepted Manuscript

show that NiO nano-particles of 30wt%Bi-20wt%Ni-O/Al_2O_3 catalyst are not dispersed on the stacked nano-particles of Al_2O_3 support but more highly dispersed as finer particles or clusters with roughly ordered rhombuses-like patterns, on specific surface of Bi_2O_3 nano-crystal particles, in agreement with considerations by using XRD measurement. As for Bi_2O_3 nano-particles, Fig. 12 (a) shows that the Bi_2O_3 nano-particles are rather uniformed with spherical shapes of average particle size: 10.1 nm. The size distribution is similar to that of Al_2O_3 support. This fact suggests that the uniformed pore size and its distribution of Al_2O_3 support controls the size of Bi_2O_3 nano-particles impregnated. And the impregnation is not pore fill-up type but pore expansion type. Furthermore, HRTEM images shown in Figs. 12 (b and c) clearly display that the lattice fringes of beta-Bi_2O_3 or alpha-Bi_2O_3 have many defect appearance. The observed HRTEM image shows a lattice spacing of 0.27 nm and 0.32 nm, corresponding to that of (201) plane and (220) of beta-Bi_2O_3 or (200) plane and (120) of alpha-Bi_2O_3, respectively. The set of lattice spacing values cannot assign each Bi_2O_3 to beta-phase or alpha-phase because each crystal is not clear enough and includes many defects. The FFT image of HRTEM shows mixed sets of diffraction dots with at least monoclinic and tetragonal structures. The result further confirms the consideration by XRD measurement that the catalyst contains mixture of beta-Bi_2O_3 and alpha-Bi_2O_3 crystals.

Catalysis Science & Technology Accepted Manuscript

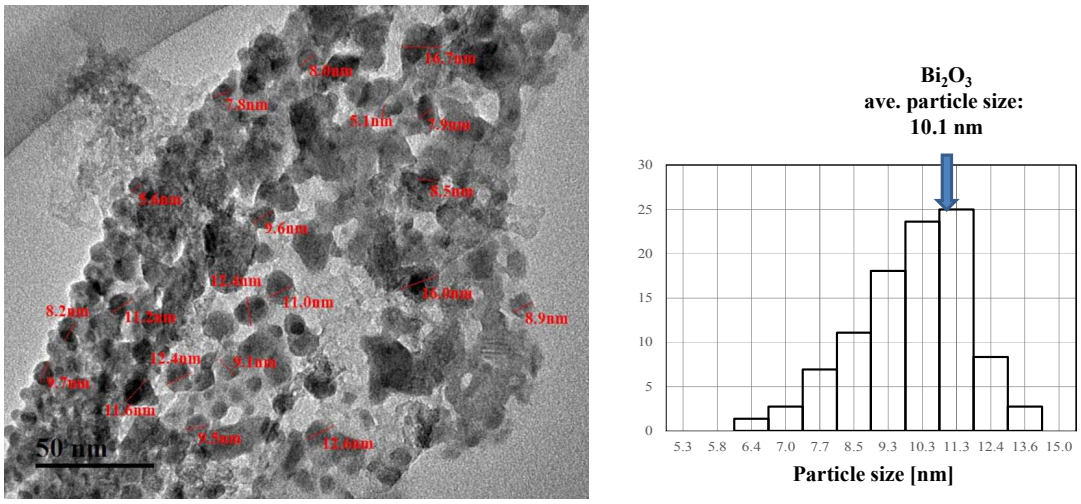

Fig. 12 (a) TEM image of 30wt%Bi-20wt%Ni-O/Al_2O_3 catalyst with measured particle size (Right: distribution of Bi_2O_3 nano-particle).

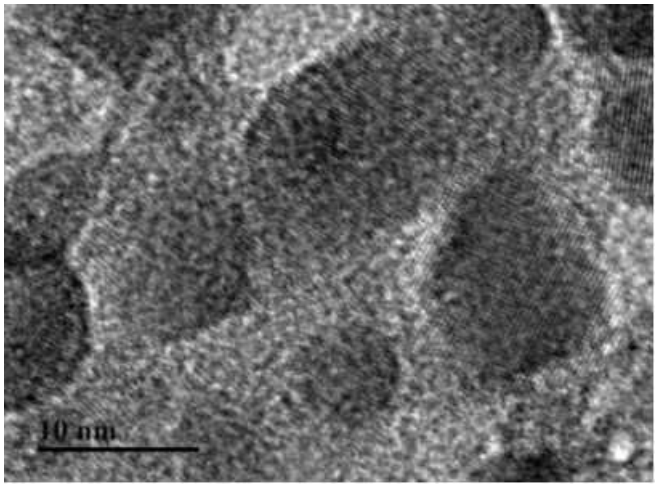

Fig. 12(b) HRTEM image of 30wt%Bi-20wt%Ni-O/Al_2O_3 catalyst

Catalysis Science & Technology Accepted Manuscript

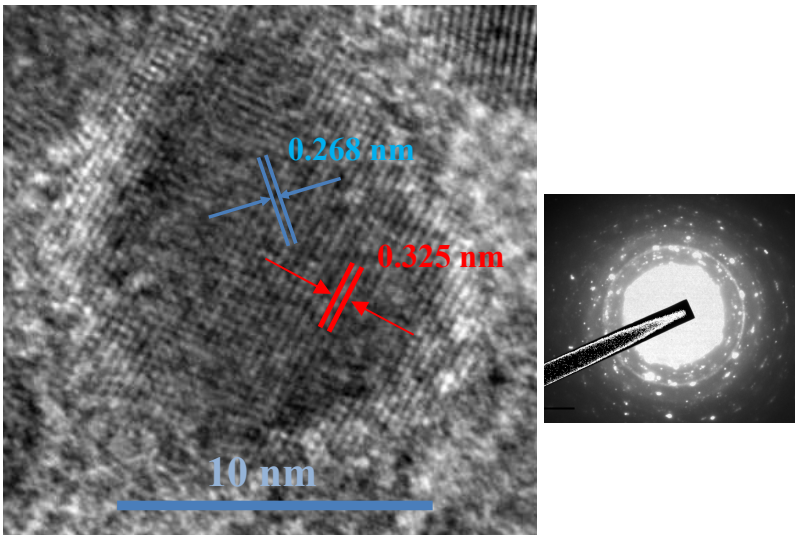

Fig. 12 (c) HRTEM image of 30wt%Bi-20wt%Ni-O/Al_2O_3 catalyst with lattice spacing values (Right: FFT image)

The most important result of the TEM observation is that three species, NiO, Bi_2O_3 and Al_2O_3 cohabit as 'hierarchical nano-particles', i.e. NiO: at the top as the finest (sub nanometer), Bi_2O_3: in the middle as ca. 10 nm size, and Al_2O_3: at ground level as stacked nano-particles serving Bi_2O_3 particles with ca. 10 nm size pores.

3.2.4 Temperature Programmed Reduction

In general for oxidative dehydrogenation of alkanes, the reaction is considered to proceed via redox mechanism, in which the reducibility (linking to re-oxidation ability) of active sites is a key factor for the catalyst activity[45]. In order to measure the reducibility of NiO-Bi_2O_3 species, TPR analyses were performed. Fig. 13 shows the TPR profiles of 30wt%Bi-20wt%Ni-O/Al_2O_3 catalysts calcined at various temperatures. The reduction peak maxima as well as the amount of H_2 uptake (mmol/g) was summarized in supporting data (Table s2). The peak position shifted with the calcination temperatures as

Catalysis Science & Technology Accepted Manuscript

shown in Fig. 13. Comparing among TPR profiles of the catalysts calcined at various temperatures, the profiles were revealed to involve four peaks, I (low), II (low-middle), III (high-middle) and IV (high) of hydrogen consumption temperature. The total and fractional H_2 uptakes to the catalysts calcined at various temperatures were changed as shown in Table s2. The total H_2 uptake changed cosine-like with the bottom at 590 ^oC calcination. The value change becomes valley shape after correction to concentration by surface area, in agreement with oxygenate formation selectivity. The low and low-middle temperature peaks decreased and the high middle temperature did not change so much with increase of calcination temperature from 550 ^oC to 590 ^oC. Reversely, the low temperature peak increased to shift to lower temperature and the low-middle temperature peak increased to lower temperature with disappearance of the high-middle, as observed in the TPR spectrum of the 650 ^oC calcined catalyst. The low temperature peak again decreased to shift to high temperature in the 750 ^oC calcined catalyst. These changes of reducibility is considered to relate to the state of NiO and Bi_2O_3 including these nano-particle contact with each other. Based on the previous TPR work for Ni and Bi monometallic oxide catalysts, the four TPR peaks were assigned. The first two reduction peaks (500-650 ^oC) are attributed to NiO species, while the third reduction peak is ascribed to the reduction of Ni and Bi oxide species. The fourth peak corresponds to isolated bismuth oxide species. The NiO of sample 30wt%Bi-20wt%Ni-O/Al_2O_3 calcined at 590 ^oC calcined catalyst behaves the most steadily as an active one. As the result, high selectivity to butadiene and low oxygenate and partial oxidation products was observed (Fig. 5).

Catalysis Science & Technology Accepted Manuscript

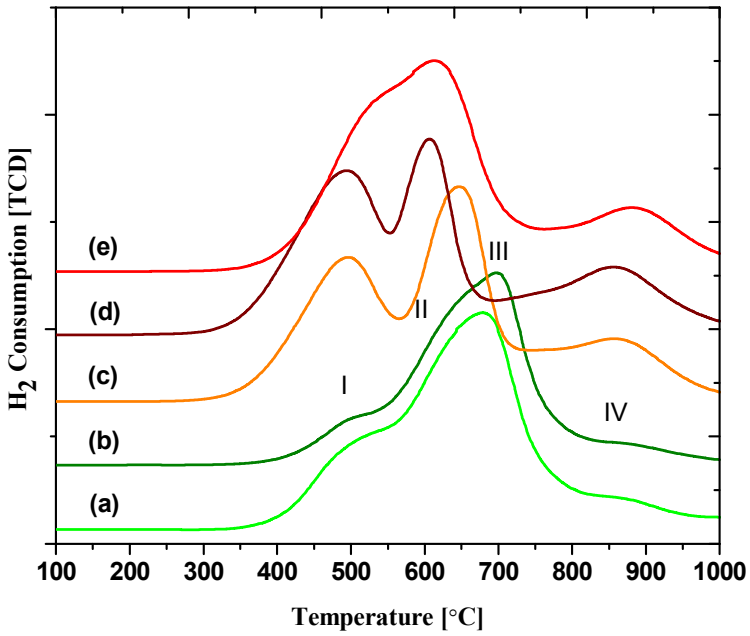

Fig. 13 TPR profiles with various calcination temperatures. (a) 550 ^{o}C, (b) 590 ^{o}C, (c) 650 ^{o}C, (d) 700 ^{o}C and (e) 750 ^{o}C.

On the contrarily, the NiO species of the catalysts calcined at 550 ^{o}C and more than 650 ^{o}C look like to work not only as active hydrogen consumer and supplier to Bi_2O_3 but also reversely as active oxygen supplier and exit from Bi_2O_3 for oxygenate production (Fig. 5).

Based on the reaction results, the mechanism of dehydrogenation performed by redox cycle of nickel supported by bismuth oxide species are shown in Fig. 14. It is well known that nickel oxide species are easily reducible from Ni^{2+} to Ni^{0} state by hydrocarbon reactant in non-oxidative dehydrogenation. The nickel oxide redox system is better stabilized on the mixed phase of bismuth oxide as nanoparticle cohabitation. During the Ni redox cycle, many defects are created in Ni species as fine nanoparticles. The controlled O^{2-} supply from bismuth oxide to the Ni defect makes the redox system of

Catalysis Science & Technology Accepted Manuscript

Ni^{2+} to Ni^{+} more efficient.

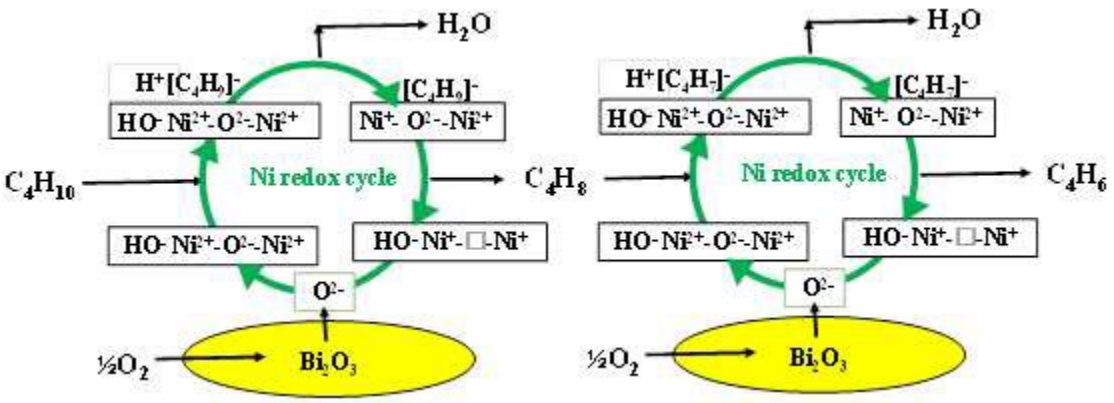

Fig. 14. Mechanism of the dehydrogenation performed by redox cycle of Ni (Ni-Bi bimetallic) species.

Conclusively as for the preferable reducibility of the catalyst to selective butadiene production, NiO species are reduced only by n-butane and butene intermediate and re-oxidized by oxygen species without supply of oxygen species active to oxygenate formation. There was no carbon deposition observed as measured from carbon analysis for spent catalysts, though very remarkable amount of carbon deposition was observed in the spent catalysts served to the condition of oxygen absence. Without oxygen the Ni redox cycle does not work well and excessively reduced Ni species cause the carbon deposition

Therefore, the catalyst calcined at 590 ^{o}C is considered to be the nearest one due to the cohabitation of 'hierarchical nano-particles'. The 'hierarchical nano-particle' cohabitation is not yet established well at the catalyst calcined at 550 ^{o}C and the calcinations at higher than 650 ºC disintegrate the hierarchy to unify the nano-particle species, in which active oxygen species assigned to low and low-middle peaks may move freely to behave as an oxygenate maker.

Catalysis Science & Technology Accepted Manuscript

3.2.5 Temperature Programmed Desorption (NH_3/CO_2)

The acidity studied by NH_3-temperature programmed desorption technique (NH_3-TPD) on 30wt%Bi-20wt%Ni-O/Al_2O_3 catalysts calcined at various temperatures are shown in supporting data Fig. s5 (A). The acid amount deconvolved to the three strength groups were calculated from the deconvolved amounts of the desorbed NH_3. The results are presented in Table 4. The NH_3-TPD spectra showed an initial desorption peak around 180 °C accompanied with a broad desorption peak extending up to 500 °C. The 180 °C peak was assigned as a weak acid fraction and the broad peak as a mixture of the moderate with the strong. In the case of the calcined at 550 °C, the presence of weak, medium and strong acid sites are clearly observed (Table 4). In the cases of the catalyst calcined at temperatures higher than 550 °C, all three types of acidity decreased with the increase of calcination temperature. The decrease ratio is the maximum from 550 °C to 590 °C of the calcination temperature, where each acid amount becomes nearly half relative to 2/3 from 590 °C to 750 °C. Since surface areas of the two catalysts calcined at 550 °C and 590 °C as shown in Table 3 nearly equal, the acid sites of the 550 °C calcined is considered to cause the low selectivity of dehydrogenation and butadiene production. And the selectivity decreases of dehydrogenation and butadiene production with the increase of calcination temperature from 590 °C to 750 °C is thought to be due to the increase of acid concentration because surface area decreased in more than degree of acid amount decrease. Therefore, the selectivity of butadiene production is not controlled by the acid amount but by the acid concentration balanced to the base concentration.

The basicity of samples was measured using CO_2-TPD, as shown in supporting data Fig. s5(B) and summarized in Table 4. The catalysts without the 550 °C calcined

Catalysis Science & Technology Accepted Manuscript

showed the similar CO_2-TPD profiles with two distinct desorption peaks centered at about ca. 150 ^oC and ca. 350-450 ^oC. The low temperature desorption peak was assigned to the low-strength (weak) basic sites, which resulted from the interaction between CO_2 with weak basic surface hydroxyl groups. The desorption peaks at ca. 350-450 ^oC are probably due to high-strength (strong) basic sites. The 550 ^oC calcined catalyst showed the third peak as the middle-strength (moderate) basic sites. The increased temperature of catalyst calcination caused a volcano-type change of the strongly basic character (peak III) with the top at the 590 ^oC calcined. This behavior looks like corresponding to the selectivity change. Furthermore, the site balance of strong base to strong acid may shift into acid-rich side to cause the selectivity decrease of butadiene production.

Table 4. Temperature programmed analysis (NH_3- and CO_2-TPD) of 30wt%Bi-20wt%Ni-O/Al_2O_3 catalysts calcined at various temperatures.

Calcined Temp. (^oC)	NH_3-TPD Acid amount [mmol/g]*[1]				CO_2-TPD Base amount [mmol/g]*[2]			
	I (180^oC)	II (300^oC)	III (400^oC)	Total	I (170^oC)	II (^oC)	III (^oC)	Total
550	0.181	0.254	0.138	0.573	0.058	0.396 (325)	0.108 (450)	0.562
590	0.115	0.169	0.097	0.381	0.073	-	0.173 (450)	0.246
650	0.089	0.172	0.077	0.338	0.070	-	0.152 (425)	0.222
700	0.073	0.124	0.072	0.269	0.047	-	0.143 (350)	0.190
750	0.066	0.119	0.059	0.244	0.039	-	0.160 (340)	0.199

*[1]: I: weak acid, II: moderate acid, III: strong acid
*[2]: I: weak base, II: moderate base, III: strong base

Catalysis Science & Technology Accepted Manuscript

3.3 Modeling of reaction and catalyst

The activity and selectivity in the oxidation reactions are possibly governed either by redox character or by the acid-base properties of the catalyst and the reactants. For the selective butadiene production, selective dehydrogenation to1-butene has been revealed at the former part of the discussion. It is the well-known fact that basic catalyst works to withdraw hydrogen atom as proton selectively from alpha-position methyl carbon of n-butane. Reversely, acid catalyst withdraw hydrogen atom as hydride selectively from beta-position methylene carbon of n-butane. The dehydrogenated intermediate products, butenes are considered to be basic compounds because of their double bonds. The basicity of butadiene is less than that of butenes because the double bonds are conjugated to reduce the basicity. An effective catalyst for the butadiene production for dehydrogenated basic compounds should possess a sufficient acidic property for butene adsorption with basic sites for selective proton withdrawing. Therefore, Scheme 2 is proposed schematically as reaction route and catalyst active sites for oxidative dehydrogenation of n-butane to butadiene over Bi-Ni oxide/Al_2O_3 catalyst. Scheme 3 is shown as model of reaction and catalyst for oxidative dehydrogenation of n-butane to butadiene over Bi-Ni oxide/Al_2O_3 catalyst.

Catalysis Science & Technology Accepted Manuscript

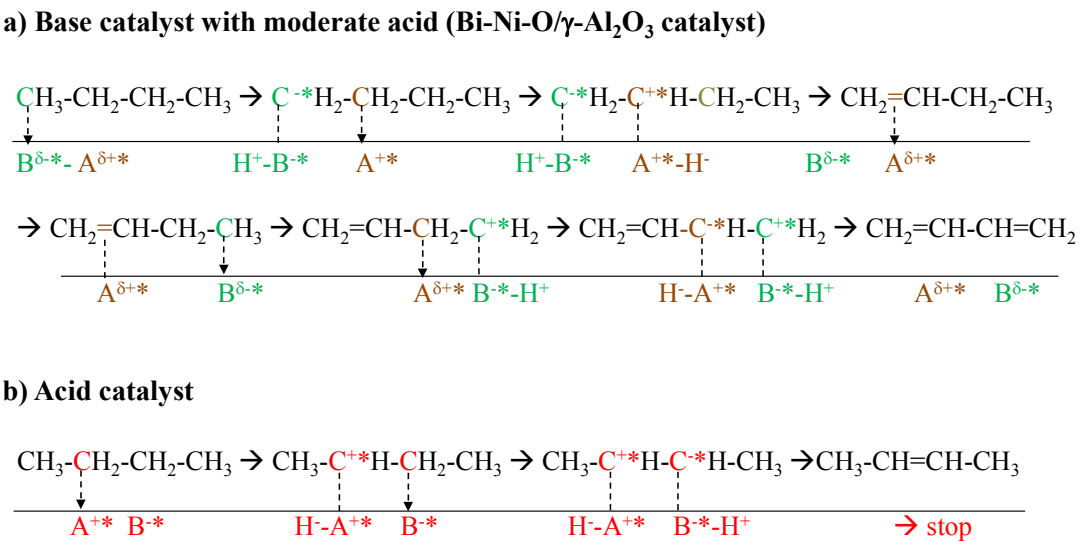

Scheme 2. Proposed reaction route and catalyst active sites for oxidative dehydrogenation of n-butane to butadiene over Bi-Ni oxide/Al_2O_3 catalyst

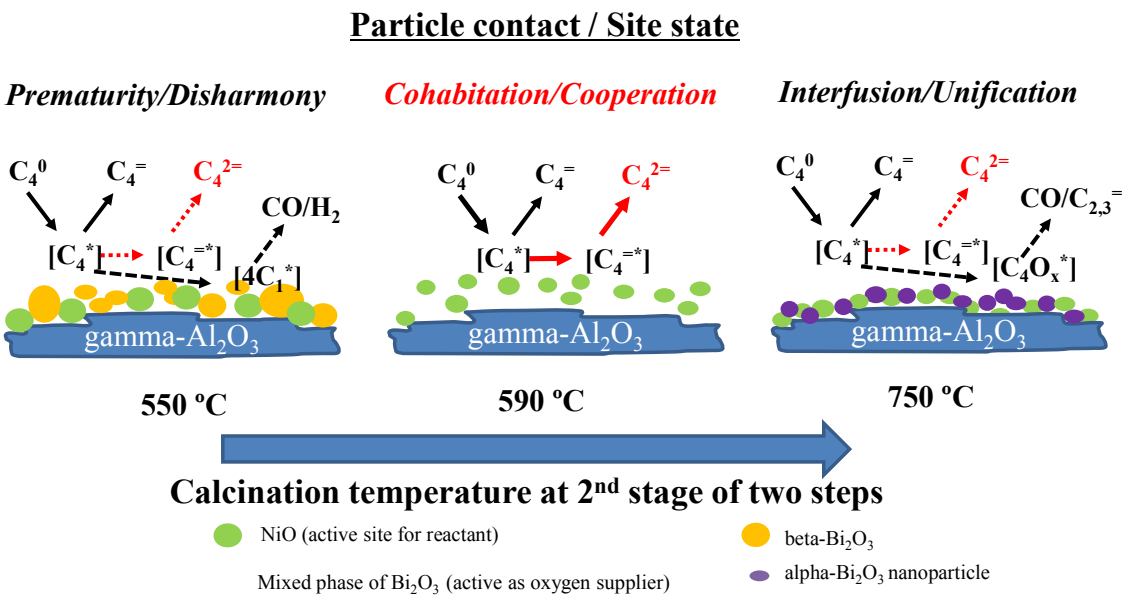

Scheme 3. Model of reaction and catalyst for oxidative dehydrogenation of n-butane to butadiene over Bi-Ni oxide/Al_2O_3 catalyst

Catalysis Science & Technology Accepted Manuscript

4. Conclusions

Influence of calcination procedure and its temperature on 30wt%Bi-30wt%Ni-O/Al_2O_3 catalyst was studied for the activity and selectivity of n-butane oxidative dehydrogenation to butadiene. The importance of the 2nd step calcination at 590 ºC for enough time was confirmed. Either the total dehydrogenation or the specific butadiene selectivity showed a volcano shape with the calcination temperature. The top along the calcination temperature existed at 590 ºC. The calcination temperature effect on the catalyst activity and selectivity for oxidative dehydrogenation of n-butane to butadiene was revealed by catalyst characterization. The characterization reveals that cohabitation as 'hierarchical nano-particles' consisting of NiO, Bi_2O_3 and Al_2O_3 are resulted from preferable calcination condition, forming the redox and acid/base system of the combined oxides with porous structure that are active and selective to the reaction.

Acknowledgement

We are grateful for the support from Ministry of Higher Education, Saudi Arabia for the establishment of the Center of Research Excellence in Petroleum Refining and Petrochemicals at King Fahd University of Petroleum and Minerals (KFUPM). The authors acknowledge Japan Cooperation Center, Petroleum (JCCP) to give the opportunity of this collaborative research.

Catalysis Science & Technology Accepted Manuscript

References

1. H.-J. Arpe, *Industrial Organic Chemistry*, WILEY=VCH Verlag GmbH & Co. KGaA, 2010.

2. H. N. Sun and J. P. Wristers and Kirk-Othmer *Encyclopaedia of Chemical Technology*, JohnWiley & Sons, Inc., 2000, 365-392.

3. J.D. Burrington, C.T. Kartisek and R.K. Grasselli, *J. Catal.,* 1980, **63**, 235-254.

4. B. P. Ajayi, B. R. Jermy, K.E. Ogunronbi, B.A. Abussaud and S. Al-Khattaf, *Catal. Today* 2012*,* **204**, 189-196.

5. B.P. Ajayi, B. R. Jermy, B.A. Abussaud and S. Al-Khattaf, *J. Porous Mater.,* 2013, **20**, 1257-1270.

6. M. Cherian, M.S. Rao, A.M. Hirt, I.E. Wachs, and G. Deo, *J Catal.,* 2002, **211**, 482-495.

7. I-C. Marcua, I. Sandulescu, and J-M.M. Millet, *J. Mol. Catal. A: Chem*., 2003, **203**, 241-250.

8. V. Murgia, E. M. F. Torres, J. C. Gottifredi and E. L. Sham, *Appl. Catal. A: Gen.,* 2006, **312**, 134-143.

9. A. P. V. Soares, L. D. Dimitrov, M. C. A. de Oliveira, L. Hilaire, M. F. Portela and R. K. Grasselli, *Appl. Catal. A: Gen.,* 2003, **253**, 191-200.

10. A. A. Lemonidou and M. Machli, *Catal. Today* 2007, **127**, 132-138.

11. D. Bhattacharyya, S. K. Bej and M. S. Rao, *Appl. Catal. A: Gen.,* 1992, **87**, 29-43.

Catalysis Science & Technology Accepted Manuscript

12. O. Rubio, J. Herguido and M. Menendez, *Chem. Eng. Sci.,* 2003, **58**, 4619-4627.

13. N. Kijima, M. Toba and Y. Yoshimura, Catal. Lett., 2009, **127**, 63-69.

14. F.J. Maldonado-Hodar, L.M. Palma Madeira and M. Farinha Portela, *J. Catal.,* 1996, **164**, 399-410.

15. F.J. Maldonado-Ho´dar, L.M. Madeira, M.F. Portela, R.M. Martin-Aranda and F. Freire, *J. Mol. Catal. A:Chem.,* 1996, **111**, 313-323.

16. M.L. Pacheco, J. Soler, A. Dejoz, J.M. L. Nieto, J. Herguido, M. Menéndeza and J. Santamaria, *Catal. Today* 2000, **61**, 101-107.

17. X. Lin, C.A. Hoel, W.M.H. Sachtler, K.R. Poeppelmeier and E. Weitz, *J Catal.,* 2009, **265**, 54-62.

18. E. Heracleous and A.A. Lemonidou, *J. Catal.,* 2010, **270**, 67-75.

19. C. Berger-Karin, J. Radnik and E. V. Kondratenko, *J. Catal.,* 2011, **280**, 116-124.

20. N.M. Sammes, G.A. Tompsett, H. Nafe and F. Aldinger, *J. Eur. Ceram. Soc.,* 1999, **19**, 1801-1826.

21. N.X. Jiang and E.D. Wachsman, *J. Am. Ceram. Soc.,* 1999, **82**, 3057-3064.

22. N.X. Jiang, E.D. Wachsman and S.H. Jung, *Solid State Ionics* 2002, **150**, 347-353.

23. C.R. Xia, Y. Zhang and M.L. Liu, *Appl. Phys. Lett.,* 2003, **82**, 901-903.

24. M.A. de la Rubia, M. Peiteado, J.F. Fernandez and A.C. Caballero, *J. Eur. Ceram. Soc.,* 2004, **24**, 1209-1212.

25. M. Gotić, S. Popović and S. Musić, *Materials Letters* 2007, **61**, 709-714.

Catalysis Science & Technology Accepted Manuscript

26. H.-O. Jungk and C. Feldmann, *J. Mater. Sci.,* 2001, **36**, 297-299.

27. G.B. Yang, Y.X. Li, Q.R. Yin, P.L. Wang and Y.B. Cheng, *Mater. Lett.,* 2002, **55**, 46-49.

28. M.M. Patil, V.V. Deshpande, S.R. Dhage and V. Ravi, *Mater. Lett.,* 2005, **59**, 2523-2525.

29. O. Monnereau, L. Tortet, P. Llewellyn, F. Rouquerol and G. Vacquier, Solid State Ionics 2003, **157**, 163-169.

30. B. Rabindran Jermy, B.P. Ajayi, B.A. Abussaud, S. Asaoka and S. Al-Khattaf, *J. Mol. Catal. A: Chem.,* 2015, **400**, 121-131.

31. H. Li, W.L. Dai and J.F. Deng, *Appl. Catal. A: Gen.,* 2001, **207**, 151-157.

32. G.Y. Wang, W.X. Zhang, H.L. Lian, D.Z. Jiang and T.H. Wu, *Appl Catal. A: Gen.,* 2003, **239**, 1-10.

33. F. Wang, Y. Xu, J. Ren and Y. Li, *Chem. Eng. Process.,* 2010, **49**, 51-58.

34. J. Medema, C. Van Stam, V. De Beer, A. Konings and D. Koningsberger, *J Catal.,* 1978, **53**, 386-400.

35. M. Abello, M. Gomez and O. Ferretti, *Appl. Catal. A: Gen.,* 2001, **207**, 421-431.

36. D. Duvenhage and N. Coville, *Appl. Catal. A: Gen.,* 2002, **233**, 63-75.

37. S. Rajagopal, J. Marzari and R. Miranda, *J Catal.,* 1995, **151**, 192-203.

38. K. Chen, S. Xie, E. Iglesia and A.T. Bell, *J Catal.,* 2000*,* **189**, 421-430.

Catalysis Science & Technology Accepted Manuscript

39. M. Abello, M. Gomez, M. Casella, O. Ferretti, M. Banares and J. Fierro, *Appl Catal. A: Gen.,* 2003, **251**, 435-447.

40. Z. Boukha, L. Fitian, M. López-Haro, M. Mora, J.R. Ruiz, C. Jiménez-Sanchidrián, G. Blanco, J.J. Calvino, G.A. Cifredo and S. Trasobares, *J Catal.,* 2010, **272**, 121-130.

41. T. Kimura, K. Sakashita and S. Asaoka, *Mater. Res. Innov.,* 2011, **15,** s101-s105.

42. T. Kimura, H. Imai, X. Li, K. Sakashita, S. Asaoka and S. Al-Khattaf, *Catal. Lett.,* 2013, **143**, 1175-1181.

43. T. Kimura, H. Imai, X. Li, K. Sakashita, S. Asaoka, M. N. Akhtar and S. Al-Khattaf, *Arab J. Sci. Eng.,* 2014, **39**, 6617-6625.

44. International Centre for Diffraction Data, Joint Committee on Powder Diffraction Standards, Powder Diffraction File, 1601 Park Lane, USA.

45. H.X. Dai, A.T. Bell and E.J. Iglesia, *J. Catal.,* 2004, **221**, 491-499.

Catalysis Science & Technology Accepted Manuscript

Influence of calcination on performance of Bi-Ni-O/gamma-alumina catalyst for *n*-butane oxidative dehydrogenation to butadiene

B. Rabindran Jermy [1], S. Asaoka [1], S. Al-Khattaf [1,2]*

Supporting data:

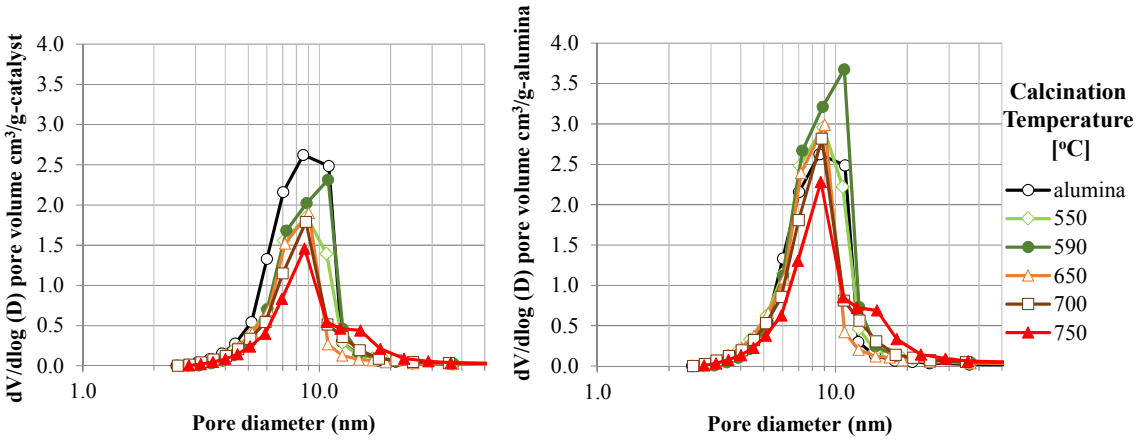

Fig. s1 Pore size distribution of catalysts with calcination temperature

Catalysis Science & Technology Accepted Manuscript

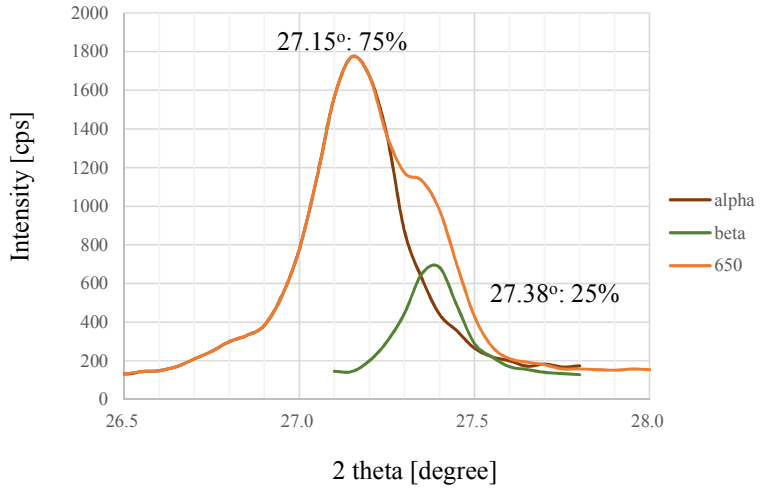

Fig.s2. XRD peak deconvolution of catalyst calcined at 650 °C

Catalysis Science & Technology Accepted Manuscript

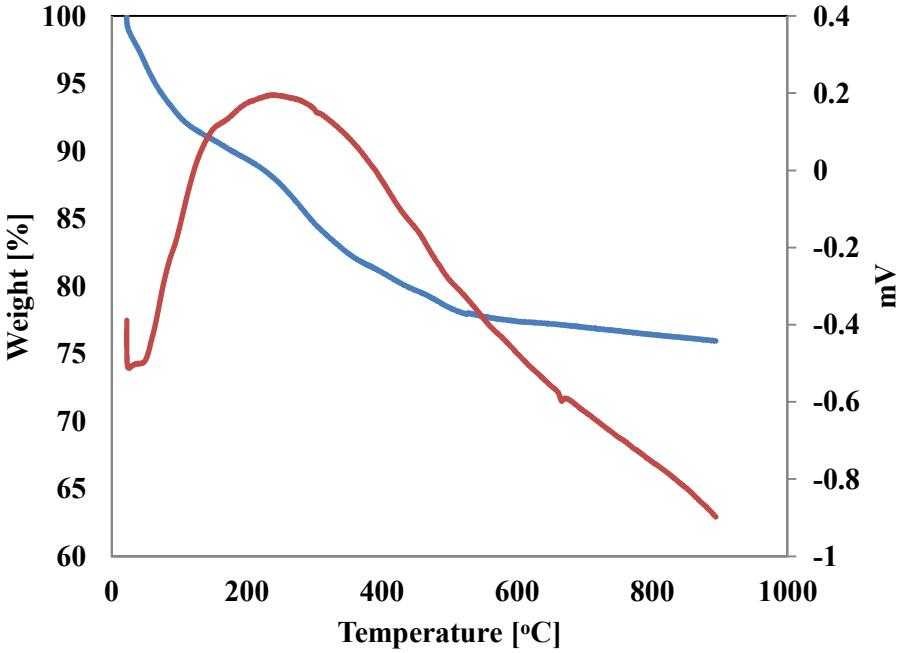

Fig. s3 TGA-DTA analysis for as-synthesized standard sample 30wt%Bi-20wt%Ni-O/Al_2O_3.

TGA-DTA analysis was carried out for as-synthesized standard sample 30wt%Bi-20wt%Ni-O /Al_2O_3. The TGA showed main weight loss occur at 250 - 350 °C (17%), and the second weight loss extends until 510 °C (5%). On the other hand, in DTA analysis, the structure change detected by XRD was not clearly observed.

Catalysis Science & Technology Accepted Manuscript

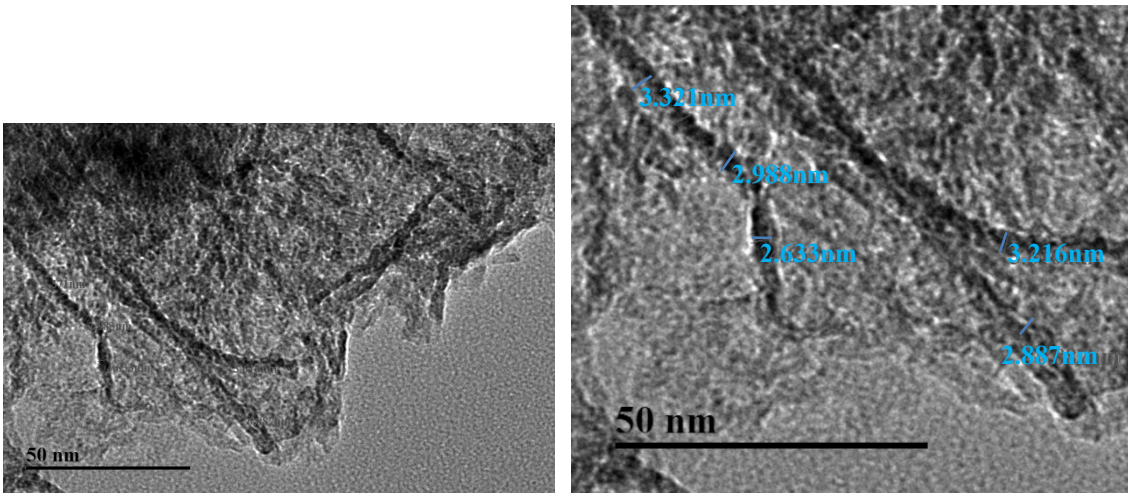

Fig. s4 TEM images of 20wt%Ni-O/Al_2O_3 catalyst (Right: for NiO size measurement)

Catalysis Science & Technology Accepted Manuscript

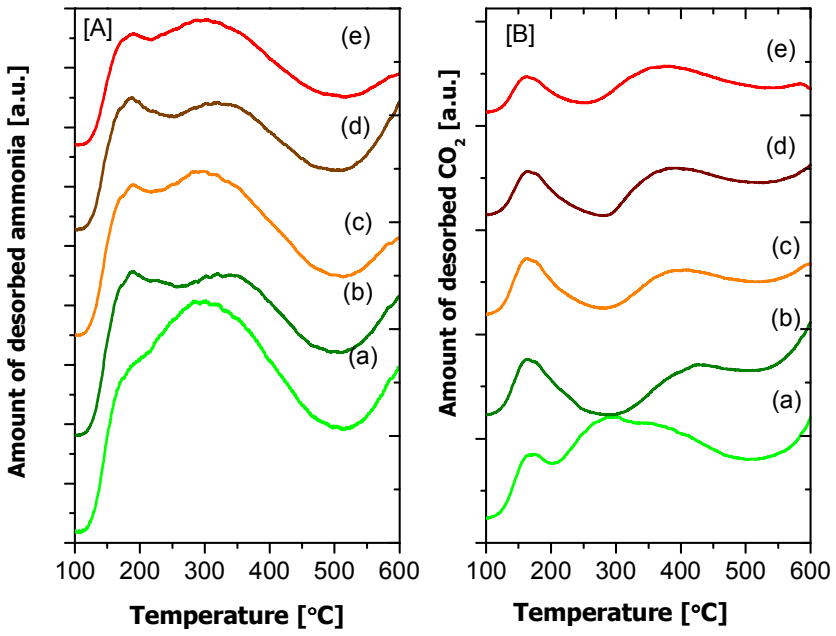

Fig. s5 TPD profile (NH_3 & CO_2) with various calcination temperatures, (a) 550 ^{o}C, (b) 590 ^{o}C, (c) 650 ^{o}C, (d) 700 ^{o}C and (e) 750 ^{o}C.

Catalysis Science & Technology Accepted Manuscript

The products found in GC with selectivity for one step and two step sample of Table 1 of manuscript is provided as supplementary table 'Table s1'.

Table s1 Products found in GC with selectivity for one step and two step sample of Table 1.

Reaction temp. [^{o}C]	400		400		450	
O_2/n-C_4H_{10} [mol/mol]	1		2		2	
Calcination step[a]	one	two	one	two	one	two
n-C_4H_{10} conversion [%]	11.8	14.1	18.4	18.3	25.9	26.9
DH selec	66.9	79.8	58.7	77.5	54.3	74.8
1-$C_4^{=}$	19.5	19.0	16.5	19.9	11.3	14.8
t-2-$C_4^{=}$	20.7	17.4	17.0	15.2	14.1	12.0
c-2-$C_4^{=}$	17.6	14.6	15.0	13.4	10.9	9.0
BD	9.1	28.8	10.2	29.0	18.0	39.0
OC selec	30.0	19.3	38.2	21.1	43.9	24.1
Ox	23.0	18.1	27.1	19.4	18.7	16.3
$C_3^{=}$	3.0	0.3	4.1	0.3	6.8	1.3
$C_2^{=}$	4.0	0.9	6.3	1.4	15.4	6.5
C_3	0.0	0.0	0.0	0.0	0.3	0.0
C_2	0.0	0.0	0.0	0.0	0.3	0.0
C_1	0.0	0.0	0.7	0.0	2.5	0.0
PO selec (CO)	3.0	0.8	3.2	1.3	1.8	1.1
S_{sum}	100.0	100.0	100.0	100.0	100.0	100.0

[a]one step: 590 ^{o}C-2h, two step: 350 ^{o}C-1h+590 ^{o}C-2h
[b] DH: dehydrogenation, BD: butadiene, OC: oxygenate and the cracked, PO: partial oxidation.

Catalysis Science & Technology Accepted Manuscript

Table s2. H_2 consumption in TPR of 30wt%Bi-20wt%Ni-O/Al_2O_3 catalysts calcined at various temperatures.

Calcination Temperature (^oC)	TPR H_2 consumption [m mol/g] (T_M[^oC])				
	I	II	III	IV	total
550	1.09 (500)	1.59 (600)	2.66 (680)	0.26 (850)	5.60
590	0.45 (500)	1.15 (600)	3.18 (700)	0.12 (850)	4.90
650	2.54 (500)	3.43 (650)	-	1.16(850)	7.13
700	2.30 (500)	3.40(630)	-	1.32 (860)	7.02
750	1.86 (500)	3.62 (620)	-	1.11 (870)	6.59

Catalysis Science & Technology Accepted Manuscript